

000 001 002 003 004 005 006 007 008 009 010 011 012 013 014 015 016 017 018 019 020 021 022 023 024 025 026 027 028 029 030 031 032 033 034 035 036 037 038 039 040 041 042 043 044 045 046 047 048 049 050 051 052 053 ZERO TUNING: UNLOCKING THE INITIAL TOKEN’S POWER TO ENHANCE LARGE LANGUAGE MODELS WITHOUT TRAINING

Anonymous authors

Paper under double-blind review

ABSTRACT

Token-level attention tuning—a class of training-free methods including Post-hoc Attention Steering (PASTA) and Attention Calibration (ACT)—has emerged as a promising way to improve frozen LLMs with interpretable interventions. However, these methods depend on auxiliary heuristics to identify “important” task-specific tokens, which can introduce bias and limit applicability when token importance is unclear or when using optimized kernels where attention maps are inaccessible. We propose a simpler and more elegant alternative: acting only on the initial token (e.g., `<BOS>` in LLaMA). We show theoretically that adding lightweight biases to this token’s attention logits systematically shifts and reshapes the downstream attention patterns—an effect amplified by its natural function as an attention sink. Our empirical analysis reveals that this tuning process can positively affect LLMs and better unlock their pretrained knowledge, with stronger effects in early layers and distinct scaling preferences across attention heads. Building on these insights, we introduce **ZeroTuning**: a training-free method that improves LLM performance by applying head-specific attention adjustments to the initial token, requiring zero parameter updates. We present two variants: a supervised mode that calibrates on validation examples, and a novel unsupervised mode that directly minimizes the model’s output entropy. Our method requires no KV-cache or decoding changes, and is kernel-agnostic (works with SDPA and FlashAttention). The method is lightweight and requires only four lines of modification to standard `LlamaAttention` code. It achieves broad gains across 15 datasets and outperforms previous, more complex methods; for instance, with Llama-3.1-8B, it yields relative improvements of 19.9% on classification, 4.5% on question answering, and 2.1% on dialogue. ZeroTuning also works out-of-the-box with quantized inference and maintains its performance improvements with increasing context lengths. Our code and runnable demo are available at <https://anonymous.4open.science/r/ZeroTuning>.

1 INTRODUCTION

Training-free methods have been widely explored to enhance Large Language Models (LLMs) performance at inference time. Among these, **token-level attention tuning** has emerged as a particularly promising direction, offering an interpretable way to steer model behavior by modifying the attention distribution without any parameter updates. Unlike fine-tuning (Hu et al., 2021; Dettmers et al., 2023) or prompt engineering (Wei et al., 2022; Wang et al., 2022), which largely treat LLMs as black boxes, attention tuning provides a transparent mechanism to guide the model’s focus. Methods such as Post-hoc Attention Steering (PASTA (Zhang et al., 2023a), AutoPASTA (Zhang et al., 2024a)), and Attention Calibration (ACT) (Yu et al., 2024) have demonstrated the power of this approach, even outperforming prompting-based techniques in complex tasks like open-domain question answering (Zhang et al., 2024a). Similar principles have been successfully applied to vision-language models to mitigate hallucinations by re-weighting attention towards image tokens (Liu et al., 2024b; Zhu et al., 2024; Wei & Zhang, 2024).

However, the efficacy of these methods is fundamentally constrained by their reliance on external, often heuristic, mechanisms to identify task-specific “important” tokens. This dependency not only

introduces the risk of bias (e.g., amplifying misleading cues) but also limits their applicability in scenarios where token importance is ambiguous or when using optimized attention kernels where attention maps are inaccessible. This critical limitation motivates a fundamental question: *Is it possible to enhance model performance by tuning a universal, task-agnostic token, thereby bypassing the need for fragile, task-specific token identification?*

```

054
055
056
057
058
059
060
061
062
063
064
065
066
067
068
069
070
071

Class LlamaAttention(nn.Module):
    def forward(self, target_layers, target_heads, scaling_factor, ...):
        # ... omitting unmodified LlamaAttention code
        # 1. Standard attention weight calculation
        attn_weights = F.softmax(torch.matmul(query_states,
                                                key_states.transpose(2, 3)), dim=-1)
        # 2. Our [ZeroTuning] Method
        if self.layer_idx in target_layers:
            # Shape: (bsz, num_heads, q_len, kv_len)
            attn_weights[:, target_heads, :, 0] *= scaling_factor
            # Re-normalize the Attention
            attn_weights[:, target_heads] =
                F.normalize(attn_weights[:, target_heads], p=1, dim=-1)
        # 3. Compute attention output
        attn_output = torch.matmul(attn_weights, value_states)
        # omitting unmodified LlamaAttention code ...

```

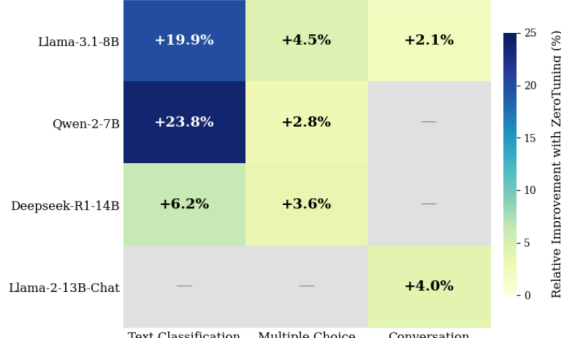


Figure 1: Overview of the **ZeroTuning** method and its effectiveness. **Left:** Our method requires only a few lines of code to scale the initial token’s attention within the model’s forward pass. **Right:** This simple intervention yields significant and consistent improvements across a variety of LLMs and tasks.

In this paper, we demonstrate that the answer is a definitive yes. The solution lies not in adding complexity, but in leveraging a ubiquitous yet often overlooked architectural artifact: the **initial token** (e.g., `<BOS>` in LLaMA). While its tendency to function as an “attention sink” is well-documented (Xiao et al., 2023; Kaul et al., 2024; Gu et al., 2024; Barbero et al., 2025), its potential as an active control lever for performance enhancement has remained largely untapped.

Our theoretical analysis reveals that modulating the attention on this single token allows for precise control – sharpening or smoothing – over the entire downstream attention distribution while preserving the relative importance of task-relevant tokens. Its natural role as an attention sink further amplifies this effect (Sec 3.1). Furthermore, we show this control can be achieved even without direct access to attention weights by modifying the initial token’s key or query states.

To validate this insight, we conducted a systematic investigation and uncovered three key findings:

1. Despite lacking semantic meaning, the initial token acts as a positive and effective control point for steering model behavior. Tuning its attention corrects the model’s biases and unlocks its pretrained knowledge with reduced output entropy. This approach consistently yields greater performance gains than tuning any other token (Sec 3.2).
2. The influence of this tuning is systemic, propagating consistently across layers. The shallow and middle layers are the most impactful, though jointly tuning all layers produces the strongest results (Sec 3.3).
3. The effect is heterogeneous across attention heads; some respond positively to increased attention (*up-effective*), while others respond negatively (*down-effective*). We show that selectively targeting the dominant head type outperforms uniform tuning (Sec 3.4, Sec 3.5).

Building on these findings, we introduce **ZeroTuning** (see Figure 1), a simple, powerful, and training-free method that recalibrates the initial token’s attention to boost LLM performance without any task-specific identification (Sec 3.6). We introduce two variants for attention calibration: a supervised mode by maximizing the accuracy on the labeled validation set, and a novel unsupervised mode by minimizing output entropy. Across a suite of 15 benchmarks, ZeroTuning achieves substantial gains on models like Llama-3.1-8B-Instruct, Llama-2-13B-Instruct, Qwen-2-7B, and Deepseek-R1-14B. For instance, it boosts Llama-3.1-8B-Instruct performance by a relative 19.9% on classification, 4.5% on question answering, and raises its MT-Bench score from 7.804 to 7.966. The method demonstrates remarkable robustness across long contexts, few-shot settings, quantization, and prompt variations. Our work not only delivers a practical tool for lightweight model enhancement but also sheds new light on a fundamental control mechanism within LLMs, advancing both inference-time optimization and model interpretability.

108 **2 RELATED WORK**
 109

110 Our work is situated at the intersection of two active research areas: inference-time attention tun-
 111 ing and the mechanistic understanding of initial tokens. A growing body of work has shown that
 112 modifying token-level attention at inference time can enhance the performance of both LLMs and
 113 VLMs (Yu et al., 2024; Zhang et al., 2023a; Liu et al., 2024b; Wei & Zhang, 2024). However, pre-
 114 vailing methods like PASTA (Zhang et al., 2023a) and Auto-PASTA (Zhang et al., 2024a), which
 115 identify and up-weight key tokens, or ACT (Yu et al., 2024), which down-weights non-initial sink
 116 tokens, fundamentally rely on heuristics to identify *task-specific* tokens. This reliance limits their
 117 universality and introduces potential biases. Concurrently, another line of research has focused on
 118 explaining *why* the initial token often becomes an "attention sink" (Xiao et al., 2023), attributing it to
 119 architectural biases and its role as a stabilizing anchor (Barbero et al., 2025; Gu et al., 2024). While
 120 these studies provide a crucial understanding of *what* the phenomenon is, the question of *how* to ac-
 121 tively and elegantly harness it for performance gains remains largely unexplored. Our work bridges
 122 this gap. We shift the focus from task-specific token identification to a universal, task-agnostic con-
 123 trol point, and move from passive observation of the initial token to a practical tuning framework
 124 that leverages its unique properties. Detailed related work is provided in Appendix A.

125 **3 UNVEILING THE POWER OF THE INITIAL TOKEN**
 126

127 In this section, we first formalize the mechanism of tuning the initial token's attention, then empiri-
 128 cally demonstrate its unique importance and dissect its effects across the model's layers and heads.
 129 This systematic analysis culminates in our proposed ZeroTuning methodology. Unless otherwise
 130 specified, all experiments use the Llama-3.1-8B-Instruct model, with setup details in Section 4.1.
 131

132 **3.1 FORMALIZING THE TUNING PROCESS**
 133

134 In a decoder-only Transformer, autoregressive generation for a sequence $\mathbf{X} = [x_0, x_1, \dots, x_{T-1}] \in$
 135 $\mathbb{R}^{d \times T}$ involves a causal self-attention mechanism. At timestep T , the query is derived from the final
 136 token representation, x_{T-1} , which attends to all preceding token representations (including itself)
 137 as keys. This process yields an attention weight distribution over the input sequence:

$$138 \quad \mathbf{a} = [a_0, a_1, \dots, a_{T-1}], \quad \text{where } a_i \geq 0 \quad \text{and} \quad \sum_{i=0}^{T-1} a_i = 1. \quad (1)$$

141 Here, a_0 is the attention score assigned to the initial token, while a_1, \dots, a_{T-1} correspond to subse-
 142 quent tokens. To control the influence of x_0 , we introduce a tuning factor $\gamma > 0$ to scale its attention
 143 and re-normalize:

$$144 \quad a'_0 = \frac{\gamma a_0}{D}, \quad a'_i = \frac{a_i}{D} \quad \text{for } i = 1, \dots, T-1, \quad (2)$$

146 where the normalization constant $D = \gamma a_0 + \sum_{i=1}^{T-1} a_i = (\gamma - 1)a_0 + 1$.

148 This rescaling preserves the relative proportions among all non-initial tokens:

$$149 \quad \frac{a'_i}{\sum_{j=1}^{T-1} a'_j} = \frac{\frac{a_i}{D}}{\sum_{j=1}^{T-1} \frac{a_j}{D}} = \frac{a_i}{\sum_{j=1}^{T-1} a_j}, \quad \text{for } i \geq 1, \quad (3)$$

152 but compresses or expands their differences as

$$154 \quad a'_i - a'_j = \frac{a_i - a_j}{D} = \frac{a_i - a_j}{(\gamma - 1)a_0 + 1}, \quad \text{for } i, j \geq 1. \quad (4)$$

156 Intuitively, $\gamma > 1$ amplifies a_0 , flattening the remaining distribution, while $\gamma < 1$ suppresses a_0 ,
 157 sharpening it. Theoretically, the magnitude of this effect is governed by the initial token's own
 158 attention weight, a_0 . We define this effect, $E_{\text{diff},i,j}$, as the change in attention difference between
 159 any two non-initial tokens i and j :

$$161 \quad E_{\text{diff},i,j} = |(a'_i - a'_j) - (a_i - a_j)| = |a_i - a_j| \left| \frac{1}{(\gamma - 1)a_0 + 1} - 1 \right| = |a_i - a_j| \frac{|\gamma - 1|a_0}{(\gamma - 1)a_0 + 1}. \quad (5)$$

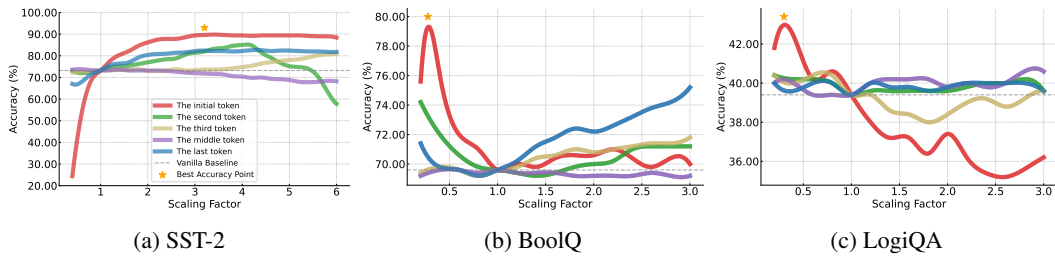
162 To analyze how $E_{\text{diff},i,j}$ varies with a_0 , we take its partial derivative with respect to a_0 :
 163

$$\frac{\partial E_{\text{diff},i,j}}{\partial a_0} = |a_i - a_j| |\gamma - 1| \cdot \frac{1}{((\gamma - 1)a_0 + 1)^2}. \quad (6)$$

167 Given that $|a_i - a_j| |\gamma - 1| \geq 0$ and the denominator $((\gamma - 1)a_0 + 1)^2 = D^2 > 0$, the derivative
 168 is non-negative. Thus, $E_{\text{diff},i,j}$ is a monotonically non-decreasing function of a_0 . In any non-trivial
 169 case ($\gamma \neq 1$ and $a_i \neq a_j$), the relationship is strictly increasing. A detailed proof and visualization
 170 are in Appendix C.

171 **This result provides a crucial insight:** *the larger the initial token’s attention score (a_0), the more*
 172 *powerful it becomes as a lever for controlling the entire attention distribution.* Since prior work has
 173 established that initial tokens are natural *attention sinks* (Barbero et al., 2025), they are inherently
 174 potent control points for this tuning process.
 175

176 3.2 THE UNIQUE IMPORTANCE OF THE INITIAL TOKEN

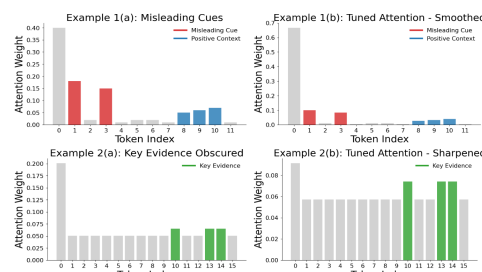


187 Figure 2: Impact of attention scaling factor γ on different token positions across three tasks: (a) SST-
 188 2, (b) BoolQ, and (c) LogiQA. Modifying the initial token’s attention consistently yields significant
 189 accuracy improvements, often surpassing adjustments to other tokens.

190 Given the special role of the initial token, we first investigate a key empirical question: (a) Does
 191 tuning its attention positively impact performance on downstream tasks? (b) Is this position more
 192 effective and influential than others? To investigate, we conduct a controlled experiment in which
 193 we uniformly scale the attention scores of a single token position across all heads and layers using
 194 a scaling factor γ . We evaluate the resulting performance on three downstream tasks: SST-2,
 195 BoolQ, and LogiQA. For comparison, we repeat the same procedure for other positions, including
 196 the second, third, middle ($\lfloor T/2 \rfloor$), and final tokens. As shown in Figure 2, tuning the attention of the
 197 initial token consistently yields the largest and most stable performance gains across all tasks. Inter-
 198 interestingly, performance varies with the direction of tuning: tasks like SST-2 benefit from up-scaling
 199 ($\gamma > 1$), while BoolQ and LogiQA improve with down-scaling ($\gamma < 1$).
 200

201 Previous work has identified the initial token as
 202 an *attention sink* that helps prevent over-mixing of
 203 information during autoregressive generation (Gu
 204 et al., 2024; Barbero et al., 2025). Our empirical
 205 results extend this understanding, showing that tuning
 206 the initial token’s attention beneficially reshapes the
 207 distribution over subsequent tokens and, in turn, im-
 208 proves model performance across tasks. This benefi-
 209 cial effect can be understood from two perspectives.

210 **1. Correcting Biases.** The tuning process counter-
 211 acts reasoning flaws caused by pretrained attention
 212 biases for each dataset, as visualized in Figure 3. Our error analysis reveals a clear pattern: **(a)**
 213 **Up-scaling** ($\gamma > 1$) benefits tasks requiring *holistic context integration*. It flattens the attention dis-
 214 tribution, preventing the model from over-focusing on misleading local cues. For instance, in SST-2
 215 sentiment analysis (see Appendix F), LLMs often fixate on isolated negative keywords while ign-
 216 oring the surrounding positive context. Increasing the initial token’s attention promotes a more bal-
 217 anced, global understanding, thereby correcting such biased predictions. **(b) Down-scaling** ($\gamma < 1$)



218 Figure 3: The impact of the tuning.

benefits tasks demanding *sharp focus* on critical evidence. It amplifies the relative weights of non-initial tokens, helping the model pinpoint key details in a diffuse context. In long-context tasks like BoolQ, a model’s focus can become diluted, failing to locate the precise text segment containing the answer. Reducing the initial token’s attention sharpens the model’s focus on this salient information.

2. Reducing Predictive Uncertainty.

The tuning process can be viewed through the lens of output entropy, a proxy for model uncertainty. As illustrated in Figure 4, a clear inverse correlation emerges: the scaling factor that minimizes entropy consistently aligns with the factor that maximizes accuracy. This suggests our method better unlocks the model’s pretrained knowledge, leading to more confident and correct predictions.

3.3 LAYER-WISE ANALYSIS OF INITIAL TOKEN SCALING

To understand the propagation of this effect, we examine how its effect varies when applied selectively across different layers. Following prior work on layer functionality in transformer-based models (Jin et al., 2024; Zhang et al., 2024b), we divide the 32 layers of Llama-3.1-8B-Instruct into three groups: **shallow** (Layers 1–10), **middle** (Layers 11–21), and **deep** (Layers 22–31). We then perform independent attention scaling experiments for each group on six tasks: BoolQ, SST-2, SST-5, MR, LogiQA, and MathQA. Based on earlier findings, we apply a scaling range of [0, 1] for BoolQ and LogiQA, and [1, 2] for the remaining tasks.

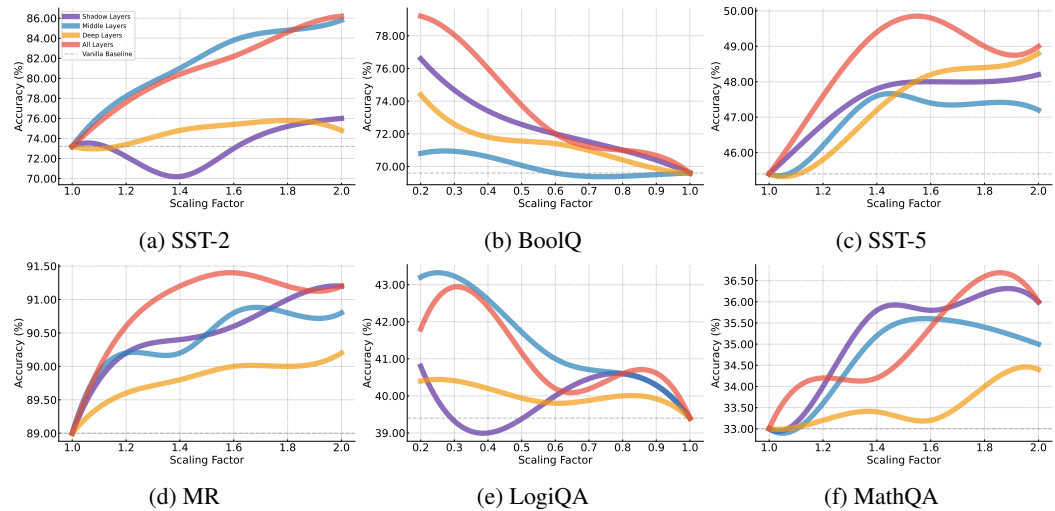
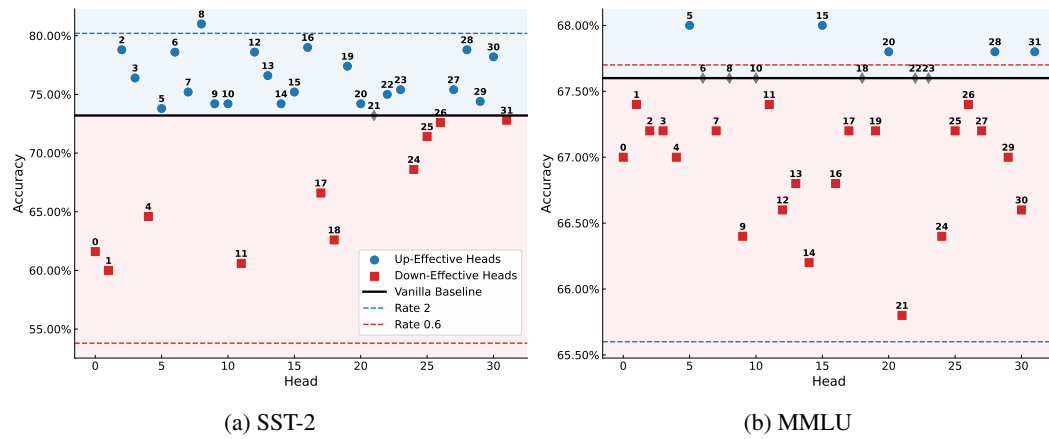


Figure 5: Accuracy trends when scaling the initial token’s attention across different layer groups: shallow (Layers 1–10), middle (Layers 11–21), and deep (Layers 22–31). Different depths exhibit a consistent accuracy trend with varying magnitudes.

As shown in Figure 5, tuning yields consistent trends at any depth (i.e., accuracy changes similarly with scaling regardless of depth), and jointly tuning all layers amplifies these benefits, often resulting in the highest accuracy. However, the magnitude of improvement varies. In most cases, tuning the shallow and middle layers leads to greater accuracy than tuning the deep layers.

Prior studies have found that early and middle layers mainly support representation learning and knowledge integration, while deep layers focus on task-specific reasoning over aggregated features (Chen et al., 2024; Jin et al., 2025). Therefore, we argue that the tuning process more effectively reshapes the representational space in shallow and middle layers, promoting better downstream performance and reducing uncertainty.

270 3.4 ANALYZING THE ROLE OF THE INITIAL TOKEN ACROSS ATTENTION HEADS
271

287 Figure 6: Accuracy of scaling the initial token’s attention in individual heads using $\gamma = 1.5$ across
288 (a) SST-2, (b) BoolQ, (c) MMLU, and (d) MathQA. Results reveal heterogeneous behavior among
289 heads, motivating head-specific tuning strategies.

290 Unlike layers passing information sequentially, attention heads operate in parallel and contribute
291 independently via concatenation. It remains unclear how they differ in response to the initial token.
292 To investigate this, we increase the initial token’s attention of each head individually by applying
293 $\gamma = 1.5$, and evaluate the model’s performance on SST-2 and MMLU. For comparison, we also
294 evaluate (i) no scaling ($\gamma = 1$), (ii) uniform up-scaling ($\gamma = 1.5$) across all heads, and (iii) uniform
295 down-scaling ($\gamma = 0.6$) across all heads.

296 As shown in Figure 6, attention heads exhibit distinct behaviors in response to initial token am-
297 plification. We categorize heads as *up-effective* if this modification improves performance, and
298 *down-effective* if it results in performance degradation. Interestingly, the relative proportions of
299 up-effective and down-effective heads vary across datasets, which in turn explains the observed dif-
300 ferences in response to uniform scaling. For example, SST-2 contains more up-effective heads and
301 thus benefits from uniform up-scaling. In contrast, MMLU has a higher proportion of down-effective
302 heads, making down-scaling more effective than up-scaling.

303 These results align with prior studies showing that attention heads specialize into distinct functional
304 roles during pretraining (Zheng et al., 2024b; Guo et al., 2024), such as global retrieval, structural
305 parsing, option discrimination, and negation sensitivity. We propose that these functional differ-
306 ences may explain the variable impact of initial token attention scaling, with some heads supporting
307 broad global reasoning and others focusing on salient tokens. This interpretation requires further
308 exploration in future work.

309 3.5 EVALUATING HEAD-SPECIFIC TUNING STRATEGIES
310

311 Given the diversity in head responses, we investigate whether head-specific tuning offers greater
312 effectiveness than uniform tuning. Specifically, we compare four strategies: (i) uniform scaling of
313 all heads (ALL), (ii) scaling only up-effective heads (UP), (iii) scaling only down-effective heads
314 (DOWN), and (iv) a hybrid strategy (UP+DOWN) that scales up-effective heads to a fixed optimal
315 value and tunes down-effective ones.

316 As shown in Figure 7, head-specific tuning (UP, DOWN) yields higher accuracy and faster conver-
317 gence compared to uniform scaling (ALL). Notably, UP is most effective when $\gamma > 1$, while DOWN
318 excels when $\gamma < 1$. Interestingly, the UP+DOWN strategy does not outperform UP or DOWN indi-
319 vidually, possibly due to the concatenative nature of attention heads and suboptimal joint scaling.

320 3.6 ZEROTUNING METHODOLOGY
321

322 Building on our empirical findings, we propose **ZeroTuning**, a method that enhances LLM per-
323 formance via head-specific attention adjustments to the initial token, without requiring task-specific

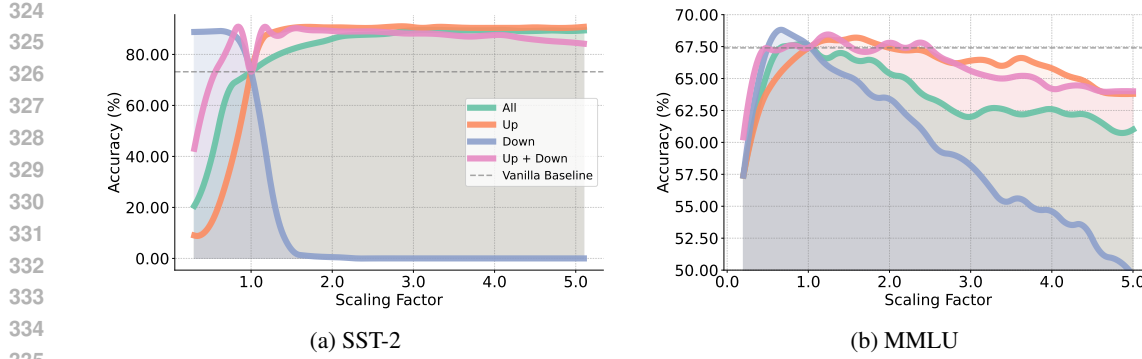


Figure 7: Accuracy comparison of different tuning strategies on (a) SST-2 and (b) MMLU. Head-specific tuning (UP, DOWN) consistently outperforms uniform scaling, validating the importance of accounting for head-level behavior.

token identification. The core methodology involves three steps: head behavior profiling, selective rescaling, and renormalization. To accomplish the first two steps, hyperparameter calibration, we introduce both supervised and unsupervised variants to cater to different application scenarios.

Supervised Calibration Consistent with standard practices in inference-time adaptation (Yu et al., 2024; Zhang et al., 2023a; 2024a), our primary approach utilizes a labeled calibration set (e.g., validation examples) to perform:

1. **Head Behavior Profiling:** Assessing each attention head’s sensitivity to the initial token’s attention scaling. A head is classified as *up-effective* if increased attention improves accuracy, and *down-effective* otherwise.
2. **Selective Rescaling:** Applying a scaling factor γ , identified by searching for the value that maximizes accuracy on the calibration set, exclusively to the dominant head type (i.e., the most numerous group).

Unsupervised Calibration via Entropy Minimization To mitigate the reliance on labeled data, we propose a novel unsupervised calibration strategy. Based on our finding that a model’s output entropy strongly correlates with its accuracy (Section 3.2), this variant does not require any labeled calibration or validation set. Instead, it identifies the optimal heads and scaling factor γ by minimizing the average next-token prediction entropy over a batch of unlabeled inputs. Crucially, the unlabeled inputs can be obtained in two practical ways: (i) in an offline setting, by running Zero-Tuning on a held-out, unlabeled corpus from the same domain; or (ii) in a test-time adaptation style, by performing entropy-based search over the current batch of test-time queries. We provide a more detailed analysis of this unsupervised variant in Appendix E.

Finally, the third step, **Renormalization**, is applied in both variants by re-normalizing the scaled attention scores via the softmax function to maintain a valid probability distribution. For optimized attention implementations (e.g., SDPA, Flash Attention) where direct score modification is infeasible, ZeroTuning applies scaling to the query or key states. We demonstrate and show that this yields similar effects in Appendix G.

4 EXPERIMENTAL RESULTS

4.1 EXPERIMENTAL SETUP

Our evaluation includes four recent LLMs with distinct attention implementations (Llama-3.1-8B, Llama-2-13B, Qwen-2-7B, and DeepSeek-R1-14B). We test performance across 15 datasets spanning three categories: Text Classification, Multiple-Choice QA, and Multi-Round Conversation. We benchmark ZeroTuning against three methods: (1) Vanilla inference; (2) ACT (Yu et al., 2024), a sink-token down-scaling method¹; and (3) Auto-PASTA (Zhang et al., 2024a), an LLM-guided key-

¹Since ACT explicitly manipulates attention maps, we only evaluate it on Llama-3.1-8B-Instruct

378 token up-scaling method. All experiments are conducted in a zero-shot setting with greedy decoding
 379 for fair comparison. For our supervised variant and the baselines, hyperparameters are calibrated on
 380 a fixed validation set. A detailed description of all models, datasets, baselines, and implementation
 381 specifics is provided in Appendix B.

384 Table 1: Performance Comparison of Classification Tasks Across Models. The best performance in each
 385 dataset is **bolded** and the ZeroTuning method is highlighted in gray.

| Model | Method | Datasets | | | | | | | | Avg. |
|-------------------------|------------|--------------|--------------|--------------|--------------|--------------|--------------|--------------|--------------|------|
| | | SST2 | SST5 | MR | BoolQ | CB | TREC | SUBJ | | |
| Llama-3.1-8B-Instruct | Vanilla | 73.20 | 45.40 | 89.20 | 69.60 | 82.14 | 14.00 | 44.60 | 59.59 | |
| | ACT | 85.00 | 43.80 | 90.80 | 58.60 | 82.14 | 15.80 | 44.60 | 60.11 | |
| | Auto-PASTA | 89.60 | 47.20 | 91.40 | 72.60 | 83.93 | 16.00 | 45.40 | 63.73 | |
| | ZeroTuning | 91.60 | 52.00 | 92.00 | 82.40 | 89.29 | 26.20 | 66.60 | 71.44 | |
| Qwen-2-7B (SDPA) | Vanilla | 78.80 | 45.40 | 72.40 | 85.00 | 78.50 | 12.60 | 13.00 | 55.10 | |
| | ACT | — | — | — | — | — | — | — | — | |
| | Auto-PASTA | 89.00 | 47.00 | 77.70 | 85.00 | 89.29 | 14.00 | 57.00 | 65.57 | |
| | ZeroTuning | 89.60 | 47.20 | 87.40 | 86.40 | 85.71 | 26.60 | 54.40 | 68.19 | |
| Deepseek-R1-14B (Flash) | Vanilla | 91.20 | 49.40 | 89.20 | 83.40 | 89.29 | 20.80 | 50.40 | 67.67 | |
| | ACT | — | — | — | — | — | — | — | — | |
| | Auto-PASTA | 92.00 | 52.20 | 89.80 | 83.40 | 92.86 | 22.60 | 50.40 | 69.04 | |
| | ZeroTuning | 93.00 | 51.20 | 90.20 | 88.00 | 92.86 | 32.00 | 55.80 | 71.87 | |

400 Table 2: Performance Comparison of Multiple-Choice Tasks Across Models.

| Model | Method | Datasets | | | | | | | | Avg. |
|-------------------------|------------|--------------|--------------|--------------|--------------|--------------|--------------|--------------|--------------|------|
| | | MMLU | AQUA | MathQA | LogiQA | CQA | PIQA | ARCC | | |
| Llama-3.1-8B-Instruct | Vanilla | 67.40 | 25.69 | 33.60 | 39.40 | 77.60 | 83.60 | 84.62 | 58.84 | |
| | ACT | 67.60 | 29.64 | 33.60 | 38.00 | 77.60 | 83.00 | 84.62 | 59.15 | |
| | Auto-PASTA | 67.00 | 31.23 | 35.20 | 40.40 | 78.20 | 84.60 | 84.62 | 60.18 | |
| | ZeroTuning | 68.80 | 30.43 | 36.60 | 42.80 | 80.40 | 85.40 | 85.95 | 61.48 | |
| Qwen-2-7B (SDPA) | Vanilla | 69.80 | 36.76 | 39.20 | 45.00 | 78.80 | 85.20 | 86.96 | 63.10 | |
| | ACT | — | — | — | — | — | — | — | — | |
| | Auto-PASTA | 69.80 | 39.13 | 39.20 | 45.00 | 82.60 | 85.40 | 86.96 | 64.01 | |
| | ZeroTuning | 70.40 | 39.92 | 40.20 | 47.40 | 81.80 | 86.20 | 87.96 | 64.84 | |
| Deepseek-R1-14B (Flash) | Vanilla | 66.60 | 38.74 | 38.20 | 27.80 | 78.20 | 84.20 | 86.62 | 60.05 | |
| | ACT | — | — | — | — | — | — | — | — | |
| | Auto-PASTA | 66.60 | 38.74 | 39.40 | 28.20 | 78.20 | 84.40 | 86.62 | 60.31 | |
| | ZeroTuning | 70.00 | 39.13 | 39.80 | 35.60 | 78.60 | 85.00 | 87.29 | 62.20 | |

414 4.2 OVERALL PERFORMANCE OF ZEROTUNING

415 For a fair and direct comparison with existing supervised baselines, our main experiments focus on
 416 the supervised ZeroTuning approach.

420 **Text Classification** We first evaluate ZeroTuning on various text classification datasets using dif-
 421 ferent LLMs, as shown in Table 1. Despite tuning only a single token, ZeroTuning consistently
 422 outperforms baselines and methods that require tuning more tokens. With Llama-3.1-8B-Instruct,
 423 it achieves an average improvement of +11.71% over vanilla, with peaks of +22.00% on SUBJ and
 424 +18.40% on SST-2. It outperforms AutoPASTA by an average of 7.71%. On Qwen-2-7B, ZeroTun-
 425 ing gains +13.09%, and on Deepseek-R1-14B, it improves by +4.20%, with a notable increase of
 426 +11.20% on TREC.

427 **Domain-Specific Multiple Choice** Next, we evaluate ZeroTuning on common domain-specific
 428 multiple-choice datasets under various settings, as shown in Table 2. For Llama-3.1-8B-Instruct,
 429 it increases the average accuracy by +2.64%, with gains of +3.40% on LogiQA and +1.40% on
 430 MMLU. Qwen-2-7B gains +1.74%, and Deepseek-R1-14B gains +2.15%, with an outstanding
 431 +7.80% on LogiQA.

432 **Multi-Round Conversation** We further
 433 demonstrate ZeroTuning’s effectiveness in
 434 multi-round conversations using MT-Bench
 435 (Zheng et al., 2024a), with results in Table 3.
 436 For Llama-3.1-8B-Instruct, ZeroTuning im-
 437 proves the average score by 0.162 points (7.966
 438 vs. 7.804). For Llama-2-13B-Chat, it achieves
 439 a 0.266 points gain (6.916 vs. 6.650), showing
 440 its effectiveness in interactive settings

441

442

443 4.3 UNSUPERVISED ZEROTUNING

444

445

446 We validate the fully unsupervised variant of
 447 ZeroTuning, which eliminates the need for
 448 any labeled calibration data by minimizing the
 449 model’s average output entropy. Appendix E
 450 provides a detailed empirical validation for this
 451 approach, including visual comparisons, empirical
 452 analysis, and a breakdown of error patterns.
 453 As shown in Figure 8, this entropy-guided
 454 method achieves performance highly competitive
 455 with its supervised counterpart, extending
 456 its applicability to label-scarce scenarios.

457

458

459 5 FURTHER ANALYSIS AND KEY FINDINGS

460

461

462 **Robustness Across Diverse Conditions.** ZeroTuning demonstrates remarkable stability. It main-
 463 tains strong performance gains even when faced with: (1) long contexts padded with irrelevant dis-
 464 tractors, where it stabilizes information flow better than the vanilla model (Appendix I); (2) few-shot
 465 scenarios, where it consistently improves instruction-following and reduces invalid outputs (Ap-
 466 pendix J); (3) significant prompt variations, including missing or altered instructions (Appendix M);
 467 and (4) low-precision 4-bit and 8-bit quantization, where it partially mitigates the associated accu-
 468 racy degradation (Appendix N).

469

470

471 **Practicality and Methodological Choices.** Our method is not only robust but also highly prac-
 472 tical. We theoretically and empirically confirm that tuning key states provides a viable, kernel-
 473 agnostic alternative to direct attention score manipulation, proving effective in optimized envi-
 474 ronments like FlashAttention (Appendix G). Furthermore, ZeroTuning is adaptable to resource-
 475 constrained settings, delivering gains even with a minimal, search-free scaling approach (Ap-
 476 pendix H). We also analyze key methodological choices, showing that tuning a moderate subset
 477 of heads (40%–70%) is optimal, providing a clear and efficient configuration (Appendix L).

478

479

480 **Boundaries of Efficacy.** Finally, we analyze the method’s boundaries and potential side effects.
 481 We quantitatively demonstrate that ZeroTuning excels at correcting a model’s uncertain errors but
 482 cannot override high-confidence mistakes rooted in flawed pretrained knowledge. We also charac-
 483 terize the negative effects of extreme tuning, which provides a clearer picture of the method’s oper-
 484 ational limits (Appendix D). This positions our method as a powerful tool for unlocking a model’s
 485 latent knowledge, rather than a substitute for fine-tuning. Intriguingly, we also find that within a
 486 safe operational range, the scaling factor can modulate output diversity in a manner analogous to
 487 temperature, but with the unique ability to alter the rank-ordering of logits and thereby correct errors
 488 that temperature scaling cannot fix. This aligns with our experiments on temperature tuning, where
 489 pure temperature adjustment fails to improve benchmark performance, while ZeroTuning yields
 490 consistent gains substantially.

Table 3: MT-Bench Performance Scores for Multi-Round Conversation Across Models

| Model | First Turn | Second Turn | Average |
|------------------------------------|-----------------------|-----------------------|-----------------------|
| gpt-4 | 8.956 | 9.025 | 8.991 |
| Llama-3.1-8B-ZeroTuning | 8.294 (+0.029) | 7.638 (+0.282) | 7.966 (+0.162) |
| Gpt-3.5-turbo | 8.075 | 7.813 | 7.944 |
| claude-instant-v1 | 7.800 | 8.013 | 7.906 |
| claude-v1 | 8.150 | 7.650 | 7.900 |
| Llama-3.1-8B-vanilla | 8.265 | 7.353 | 7.804 |
| Llama-2-13B-Chat-ZeroTuning | 7.106 (+0.043) | 6.725 (+0.487) | 6.916 (+0.266) |
| Llama-2-13B-Chat-vanilla | 7.063 | 6.238 | 6.650 |

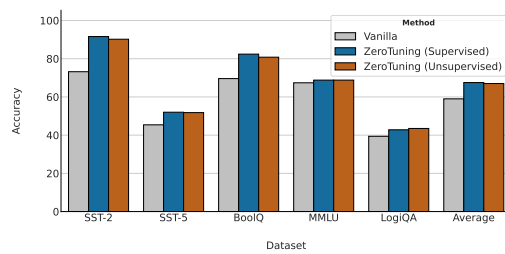


Figure 8: Performance comparison of Vanilla, Supervised, and Unsupervised ZeroTuning on Llama-3.1-8B-Instruct.

486 6 FURTHER DISCUSSION
487488 6.1 EFFICIENT CALIBRATION AND SEARCH
489490 In our current implementation, the offline search for the scaling factor γ and head selection with
491 Llama-3.1-8B takes roughly 4–5 minutes on a single GPU, and the inference-time overhead is neg-
492 ligible. **We also highlight an interesting empirical observation:** the clear U-shaped entropy curve
493 identified in Appendix E suggests that more efficient search strategies, such as Bayesian optimiza-
494 tion or simple rule-based early stopping, could further reduce calibration cost. We view this as a
495 promising direction for future optimization.496
497 6.2 ZEROTUNING AND SUPERVISED FINE-TUNING
498499 Supervised fine-tuning (SFT) remains a strong and versatile way to improve LLMs: by updating
500 parameters, it can simultaneously adjust task knowledge, instruction following, output formatting,
501 and various biases. However, this also means SFT is an indirect optimization over many intertwined
502 behaviors and typically requires more data, compute, and careful hyperparameter tuning.503 ZeroTuning takes a complementary approach. Instead of changing parameters, it directly adjusts the
504 attention pattern on the initial token, targeting the specific failure modes identified in our analysis
505 (e.g., format traps and biased attention over context tokens). This makes the intervention more
506 localized and training-free, while still being compatible with SFT.507 To study this relationship, we run a controlled experiment on BoolQ where both SFT and supervised
508 ZeroTuning use the same 500 labeled examples. We fine-tune the model with a lightweight LoRA
509 setup (rank $r = 4$, 3 epochs) and compare four configurations:510
511

| 512 Method | 513 BoolQ Accuracy |
|---------------------------------------|--------------------|
| 514 Vanilla | 69.60 |
| 515 Vanilla + SFT (LoRA) | 81.20 |
| 516 Vanilla + ZeroTuning (Ours) | 82.40 |
| 517 Vanilla + SFT + ZeroTuning (Ours) | 83.60 |

518 In this limited setting, the training-free ZeroTuning slightly outperforms our small-scale LoRA SFT,
519 and applying ZeroTuning on top of the SFT model yields the best performance. While stronger fine-
520 tuning setups (more data, higher rank, more epochs) may implicitly learn to adjust the initial-token
521 attention in a similar way, we hope our observations provide a useful lens for understanding how SFT
522 optimizes attention patterns and inspire future work on combining training-free and training-based
523 approaches.524
525 7 CONCLUSION
526527 In this work, we present a systematic analysis of tuning the initial token’s attention and propose Ze-
528 roTuning, a novel, training-free method to enhance LLMs. By recalibrating this single, task-agnostic
529 token, ZeroTuning outperforms previous methods that require task-specific tuning. It operates ef-
530 fectively in both supervised and unsupervised modes and demonstrates broad compatibility across
531 various implementations. This work advances inference-time tuning and contributes to the inter-
532 pretability of LLMs, opening new avenues for lightweight model optimization.533
534 535 REPRODUCIBILITY STATEMENT
536537 We release all code and data used in our experiments, along with detailed instructions and an easy-to-
538 run Jupyter notebook demo. Additional limitations and ablation studies are provided in the Appendix
539 to support diverse research needs.

540
541
ETHICAL STATEMENT542
543
This work does not introduce new ethical risks. All datasets used are publicly available and widely
544
adopted. We encourage responsible use of the released code and data.545
546
REFERENCES547
548
Aida Amini, Saadia Gabriel, Peter Lin, Rik Koncel-Kedziorski, Yejin Choi, and Hannaneh Ha-
549
jishirzi. Mathqa: Towards interpretable math word problem solving with operation-based for-
malisms. *arXiv preprint arXiv:1905.13319*, 2019.550
551
Federico Barbero, Álvaro Arroyo, Xiangming Gu, Christos Perivolaropoulos, Michael Bronstein,
552
Razvan Pascanu, et al. Why do llms attend to the first token? *arXiv preprint arXiv:2504.02732*,
553
2025.554
555
Yonatan Bisk, Rowan Zellers, Jianfeng Gao, Yejin Choi, et al. Piqa: Reasoning about physical com-
556
monsense in natural language. In *Proceedings of the AAAI conference on artificial intelligence*,
volume 34, pp. 7432–7439, 2020.557
558
Tom Brown, Benjamin Mann, Nick Ryder, Melanie Subbiah, Jared D Kaplan, Prafulla Dhariwal,
559
Arvind Neelakantan, Pranav Shyam, Girish Sastry, Amanda Askell, et al. Language models are
560
few-shot learners. *Advances in neural information processing systems*, 33:1877–1901, 2020.561
562
Tianxiang Chen, Zhentao Tan, Tao Gong, Yue Wu, Qi Chu, Bin Liu, Jieping Ye, and Nenghai Yu.
563
Llama slayer 8b: Shallow layers hold the key to knowledge injection, 2024. URL <https://arxiv.org/abs/2410.02330>.564
565
Christopher Clark, Kenton Lee, Ming-Wei Chang, Tom Kwiatkowski, Michael Collins, and Kristina
566
Toutanova. Boolq: Exploring the surprising difficulty of natural yes/no questions. *arXiv preprint*
567
arXiv:1905.10044, 2019.568
569
Peter Clark, Isaac Cowhey, Oren Etzioni, Tushar Khot, Ashish Sabharwal, Carissa Schoenick, and
570
Oyvind Tafjord. Think you have solved question answering? try arc, the ai2 reasoning challenge.
arXiv preprint arXiv:1803.05457, 2018.571
572
Marie-Catherine De Marneffe, Mandy Simons, and Judith Tonhauser. The commitmentbank: In-
573
vestigating projection in naturally occurring discourse. In *proceedings of Sinn und Bedeutung*,
volume 23, pp. 107–124, 2019.574
575
DeepSeek-AI, Daya Guo, Dejian Yang, Haowei Zhang, Junxiao Song, Ruoyu Zhang, Runxin Xu,
576
Qihao Zhu, Shirong Ma, Peiyi Wang, Xiao Bi, Xiaokang Zhang, Xingkai Yu, Yu Wu, Z. F. Wu,
577
Zhibin Gou, Zhihong Shao, Zhuoshu Li, Ziyi Gao, Aixin Liu, Bing Xue, Bingxuan Wang, Bochao
578
Wu, Bei Feng, Chengda Lu, Chenggang Zhao, Chengqi Deng, Chenyu Zhang, Chong Ruan,
579
Damai Dai, Deli Chen, Dongjie Ji, Erhang Li, Fangyun Lin, Fucong Dai, Fuli Luo, Guangbo Hao,
580
Guanting Chen, Guowei Li, H. Zhang, Han Bao, Hanwei Xu, Haocheng Wang, Honghui Ding,
581
Huajian Xin, Huazuo Gao, Hui Qu, Hui Li, Jianzhong Guo, Jiashi Li, Jiawei Wang, Jingchang
582
Chen, Jingyang Yuan, Junjie Qiu, Junlong Li, J. L. Cai, Jiaqi Ni, Jian Liang, Jin Chen, Kai
583
Dong, Kai Hu, Kaige Gao, Kang Guan, Kexin Huang, Kuai Yu, Lean Wang, Lecong Zhang,
584
Liang Zhao, Litong Wang, Liyue Zhang, Lei Xu, Leyi Xia, Mingchuan Zhang, Minghua Zhang,
585
Minghui Tang, Meng Li, Miaojun Wang, Mingming Li, Ning Tian, Panpan Huang, Peng Zhang,
586
Qiancheng Wang, Qinyu Chen, Qiushi Du, Ruiqi Ge, Ruisong Zhang, Ruizhe Pan, Runji Wang,
587
R. J. Chen, R. L. Jin, Ruyi Chen, Shanghao Lu, Shangyan Zhou, Shanhuang Chen, Shengfeng
588
Ye, Shiyu Wang, Shuiping Yu, Shunfeng Zhou, Shuting Pan, S. S. Li, Shuang Zhou, Shaoqing
589
Wu, Shengfeng Ye, Tao Yun, Tian Pei, Tianyu Sun, T. Wang, Wangding Zeng, Wanjia Zhao, Wen
590
Liu, Wenfeng Liang, Wenjun Gao, Wenqin Yu, Wentao Zhang, W. L. Xiao, Wei An, Xiaodong
591
Liu, Xiaohan Wang, Xiaokang Chen, Xiaotao Nie, Xin Cheng, Xin Liu, Xin Xie, Xingchao Liu,
592
Xinyu Yang, Xinyuan Li, Xuecheng Su, Xuheng Lin, X. Q. Li, Xiangyue Jin, Xiaoqin Shen, Xi-
593
aoshia Chen, Xiaowen Sun, Xiaoxiang Wang, Xinnan Song, Xinyi Zhou, Xianzu Wang, Xinxia
Wang, Y. K. Li, Y. Q. Wang, Y. X. Wei, Yang Zhang, Yanhong Xu, Yao Li, Yao Zhao, Yaofeng
Sun, Yaohui Wang, Yi Yu, Yichao Zhang, Yifan Shi, Yiliang Xiong, Ying He, Yishi Piao, Yisong
Wang, Yixuan Tan, Yiyang Ma, Yiyuan Liu, Yongqiang Guo, Yuan Ou, Yuduan Wang, Yue Gong,

594 Yuheng Zou, Yujia He, Yunfan Xiong, Yuxiang Luo, Yuxiang You, Yuxuan Liu, Yuyang Zhou,
 595 Y. X. Zhu, Yanhong Xu, Yanping Huang, Yaohui Li, Yi Zheng, Yuchen Zhu, Yunxian Ma, Ying
 596 Tang, Yukun Zha, Yuting Yan, Z. Z. Ren, Zehui Ren, Zhangli Sha, Zhe Fu, Zhean Xu, Zhenda
 597 Xie, Zhengyan Zhang, Zhewen Hao, Zhicheng Ma, Zhigang Yan, Zhiyu Wu, Zihui Gu, Zijia Zhu,
 598 Zijun Liu, Zilin Li, Ziwei Xie, Ziyang Song, Zizheng Pan, Zhen Huang, Zhipeng Xu, Zhongyu
 599 Zhang, and Zhen Zhang. Deepseek-r1: Incentivizing reasoning capability in llms via reinforce-
 600 ment learning, 2025. URL <https://arxiv.org/abs/2501.12948>.

601 Tim Dettmers, Artidoro Pagnoni, Ari Holtzman, and Luke Zettlemoyer. Qlora: Efficient finetuning
 602 of quantized llms. *ArXiv*, abs/2305.14314, 2023. URL <https://api.semanticscholar.org/CorpusID:258841328>.

603 Aaron Grattafiori, Abhimanyu Dubey, Abhinav Jauhri, Abhinav Pandey, Abhishek Kadian, Ahmad
 604 Al-Dahle, Aiesha Letman, Akhil Mathur, Alan Schelten, Alex Vaughan, et al. The llama 3 herd
 605 of models. *arXiv preprint arXiv:2407.21783*, 2024.

606 Xiangming Gu, Tianyu Pang, Chao Du, Qian Liu, Fengzhuo Zhang, Cunxiao Du, Ye Wang, and
 607 Min Lin. When attention sink emerges in language models: An empirical view. *arXiv preprint
 608 arXiv:2410.10781*, 2024.

609 Tianyu Guo, Druv Pai, Yu Bai, Jiantao Jiao, Michael I Jordan, and Song Mei. Active-dormant
 610 attention heads: Mechanistically demystifying extreme-token phenomena in llms. *arXiv preprint
 611 arXiv:2410.13835*, 2024.

612 Dan Hendrycks, Collin Burns, Steven Basart, Andy Zou, Mantas Mazeika, Dawn Song, and
 613 Jacob Steinhardt. Measuring massive multitask language understanding. *arXiv preprint
 614 arXiv:2009.03300*, 2020.

615 J. Edward Hu, Yelong Shen, Phillip Wallis, Zeyuan Allen-Zhu, Yuanzhi Li, Shean Wang, and
 616 Weizhu Chen. Lora: Low-rank adaptation of large language models. *ArXiv*, abs/2106.09685,
 617 2021. URL <https://api.semanticscholar.org/CorpusID:235458009>.

618 Mingyu Jin, Qinkai Yu, Jingyuan Huang, Qingcheng Zeng, Zhenting Wang, Wenyue Hua, Haiyan
 619 Zhao, Kai Mei, Yanda Meng, Kaize Ding, et al. Exploring concept depth: How large language
 620 models acquire knowledge and concept at different layers? *arXiv preprint arXiv:2404.07066*,
 621 2024.

622 Mingyu Jin, Qinkai Yu, Jingyuan Huang, Qingcheng Zeng, Zhenting Wang, Wenyue Hua, Haiyan
 623 Zhao, Kai Mei, Yanda Meng, Kaize Ding, Fan Yang, Mengnan Du, and Yongfeng Zhang. Explor-
 624 ing concept depth: How large language models acquire knowledge and concept at different layers?
 625 In Owen Rambow, Leo Wanner, Marianna Apidianaki, Hend Al-Khalifa, Barbara Di Eugenio,
 626 and Steven Schockaert (eds.), *Proceedings of the 31st International Conference on Compu-
 627 tational Linguistics*, pp. 558–573, Abu Dhabi, UAE, January 2025. Association for Computational
 628 Linguistics. URL <https://aclanthology.org/2025.coling-main.37/>.

629 Prannay Kaul, Chengcheng Ma, Ismail Elezi, and Jiankang Deng. From attention to activation:
 630 Unraveling the enigmas of large language models. In *The Thirteenth International Conference on
 631 Learning Representations*, 2024.

632 Xin Li and Dan Roth. Learning question classifiers. In *COLING 2002: The 19th International
 633 Conference on Computational Linguistics*, 2002.

634 Hanmeng Liu, Jian Liu, Leyang Cui, Zhiyang Teng, Nan Duan, Ming Zhou, and Yue Zhang. Logica
 635 2.0—an improved dataset for logical reasoning in natural language understanding. *IEEE/ACM
 636 Transactions on Audio, Speech, and Language Processing*, 31:2947–2962, 2023.

637 Ruiyang Liu, Haoli Bai, Haokun Lin, Yuening Li, Han Gao, Zhengzhuo Xu, Lu Hou, Jun Yao,
 638 and Chun Yuan. Intactkv: Improving large language model quantization by keeping pivot tokens
 639 intact. *arXiv preprint arXiv:2403.01241*, 2024a.

640 Shi Liu, Kecheng Zheng, and Wei Chen. Paying more attention to image: A training-free method
 641 for alleviating hallucination in lvlms. In *European Conference on Computer Vision*, pp. 125–140.
 642 Springer, 2024b.

648 Yu Lu, Jiali Zeng, Jiajun Zhang, Shuangzhi Wu, and Mu Li. Attention calibration for transformer
 649 in neural machine translation. In *Proceedings of the 59th Annual Meeting of the Association*
 650 *for Computational Linguistics and the 11th International Joint Conference on Natural Language*
 651 *Processing (Volume 1: Long Papers)*, pp. 1288–1298, 2021.

652 Bo Pang and Lillian Lee. A sentimental education: Sentiment analysis using subjectivity summarization
 653 based on minimum cuts. *arXiv preprint cs/0409058*, 2004.

654 Bo Pang and Lillian Lee. Seeing stars: Exploiting class relationships for sentiment categorization
 655 with respect to rating scales. *arXiv preprint cs/0506075*, 2005.

656 Richard Socher, Alex Perelygin, Jean Wu, Jason Chuang, Christopher D Manning, Andrew Y Ng,
 657 and Christopher Potts. Recursive deep models for semantic compositionality over a sentiment
 658 treebank. In *Proceedings of the 2013 conference on empirical methods in natural language pro-*
 659 *cessing*, pp. 1631–1642, 2013.

660 Alon Talmor, Jonathan Herzig, Nicholas Lourie, and Jonathan Berant. Commonsenseqa: A question
 661 answering challenge targeting commonsense knowledge. *arXiv preprint arXiv:1811.00937*, 2018.

662 Hugo Touvron, Louis Martin, Kevin Stone, Peter Albert, Amjad Almahairi, Yasmine Babaei, Niko-
 663 lay Bashlykov, Soumya Batra, Prajwal Bhargava, Shruti Bhosale, Dan Bikel, Lukas Blecher,
 664 Cristian Canton Ferrer, Moya Chen, Guillem Cucurull, David Esiobu, Jude Fernandes, Jeremy
 665 Fu, Wenyin Fu, Brian Fuller, Cynthia Gao, Vedanuj Goswami, Naman Goyal, Anthony Hartshorn,
 666 Saghar Hosseini, Rui Hou, Hakan Inan, Marcin Kardas, Viktor Kerkez, Madian Khabsa, Isabel
 667 Kloumann, Artem Korenev, Punit Singh Koura, Marie-Anne Lachaux, Thibaut Lavril, Jenya Lee,
 668 Diana Liskovich, Yinghai Lu, Yuning Mao, Xavier Martinet, Todor Mihaylov, Pushkar Mishra,
 669 Igor Molybog, Yixin Nie, Andrew Poulton, Jeremy Reizenstein, Rashi Rungta, Kalyan Saladi,
 670 Alan Schelten, Ruan Silva, Eric Michael Smith, Ranjan Subramanian, Xiaoqing Ellen Tan, Binh
 671 Tang, Ross Taylor, Adina Williams, Jian Xiang Kuan, Puxin Xu, Zheng Yan, Iliyan Zarov, Yuchen
 672 Zhang, Angela Fan, Melanie Kambadur, Sharan Narang, Aurelien Rodriguez, Robert Stojnic,
 673 Sergey Edunov, and Thomas Scialom. Llama 2: Open foundation and fine-tuned chat models,
 674 2023. URL <https://arxiv.org/abs/2307.09288>.

675 Xuezhi Wang, Jason Wei, Dale Schuurmans, Quoc Le, Ed H. Chi, and Denny Zhou. Self-consistency
 676 improves chain of thought reasoning in language models. *ArXiv*, abs/2203.11171, 2022. URL
 677 <https://api.semanticscholar.org/CorpusID:247595263>.

678 Jason Wei, Xuezhi Wang, Dale Schuurmans, Maarten Bosma, Ed H. Chi, F. Xia, Quoc Le,
 679 and Denny Zhou. Chain of thought prompting elicits reasoning in large language models.
 680 *ArXiv*, abs/2201.11903, 2022. URL <https://api.semanticscholar.org/CorpusID:246411621>.

681 Jinfeng Wei and Xiaofeng Zhang. Dopra: Decoding over-accumulation penalization and re-
 682 allocation in specific weighting layer. In *Proceedings of the 32nd ACM International Conference*
 683 *on Multimedia*, pp. 7065–7074, 2024.

684 G Xiao, Y Tian, B Chen, et al. Efficient streaming language models with attention sinks. *arXiv*
 685 *preprint arXiv:2309.17453*, 2023.

686 An Yang, Baosong Yang, Binyuan Hui, Bo Zheng, Bowen Yu, Chang Zhou, Chengpeng Li,
 687 Chengyuan Li, Dayiheng Liu, Fei Huang, Guanting Dong, Haoran Wei, Huan Lin, Jialong Tang,
 688 Jialin Wang, Jian Yang, Jianhong Tu, Jianwei Zhang, Jianxin Ma, Jianxin Yang, Jin Xu, Jin-
 689 gren Zhou, Jinze Bai, Jinzheng He, Junyang Lin, Kai Dang, Keming Lu, Keqin Chen, Kexin
 690 Yang, Mei Li, Mingfeng Xue, Na Ni, Pei Zhang, Peng Wang, Ru Peng, Rui Men, Ruize Gao,
 691 Runji Lin, Shijie Wang, Shuai Bai, Sinan Tan, Tianhang Zhu, Tianhao Li, Tianyu Liu, Wen-
 692 bin Ge, Xiaodong Deng, Xiaohuan Zhou, Xingzhang Ren, Xinyu Zhang, Xipin Wei, Xuancheng
 693 Ren, Xuejing Liu, Yang Fan, Yang Yao, Yichang Zhang, Yu Wan, Yunfei Chu, Yuqiong Liu,
 694 Zeyu Cui, Zhenru Zhang, Zhifang Guo, and Zhihao Fan. Qwen2 technical report, 2024. URL
 695 <https://arxiv.org/abs/2407.10671>.

696 Z Yu, Z Wang, Y Fu, et al. Unveiling and harnessing hidden attention sinks: Enhancing large
 697 language models without training through attention calibration. *arXiv preprint arXiv:2406.15765*,
 698 2024.

702 Q Zhang, C Singh, L Liu, et al. Tell your model where to attend: Post-hoc attention steering for
703 llms. *arXiv preprint arXiv:2311.02262*, 2023a.

704
705 Qingru Zhang, Xiaodong Yu, Chandan Singh, Xiaodong Liu, Liyuan Liu, Jianfeng Gao, Tuo Zhao,
706 Dan Roth, and Hao Cheng. Model tells itself where to attend: Faithfulness meets automatic
707 attention steering, 2024a. <https://arxiv.org/abs/2409.10790>.

708 Yang Zhang, Yanfei Dong, and Kenji Kawaguchi. Investigating layer importance in large language
709 models. *arXiv preprint arXiv:2409.14381*, 2024b.

710
711 Zhenyu Zhang, Ying Sheng, Tianyi Zhou, Tianlong Chen, Lianmin Zheng, Ruisi Cai, Zhao Song,
712 Yuandong Tian, Christopher Ré, Clark Barrett, et al. H2o: Heavy-hitter oracle for efficient gen-
713 erative inference of large language models. *Advances in Neural Information Processing Systems*,
714 36:34661–34710, 2023b.

715 Lianmin Zheng, Wei-Lin Chiang, Ying Sheng, Siyuan Zhuang, Zhanghao Wu, Yonghao Zhuang,
716 Zi Lin, Zhuohan Li, Dacheng Li, Eric Xing, et al. Judging llm-as-a-judge with mt-bench and
717 chatbot arena. *Advances in Neural Information Processing Systems*, 36, 2024a.

718 Zifan Zheng, Yezhaohui Wang, Yuxin Huang, Shichao Song, Mingchuan Yang, Bo Tang, Feiyu
719 Xiong, and Zhiyu Li. Attention heads of large language models: A survey, 2024b. URL <https://arxiv.org/abs/2409.03752>.

720
721 Lanyun Zhu, Deyi Ji, Tianrun Chen, Peng Xu, Jieping Ye, and Jun Liu. Ibd: Alleviating hallucina-
722 tions in large vision-language models via image-biased decoding. *ArXiv*, abs/2402.18476, 2024.
723 URL <https://api.semanticscholar.org/CorpusID:268041475>.

724
725
726
727
728
729
730
731
732
733
734
735
736
737
738
739
740
741
742
743
744
745
746
747
748
749
750
751
752
753
754
755

756 A RELATED WORK
757758 A.1 TOKEN-LEVEL ATTENTION TUNING
759

760 Token-level attention tuning typically aims to increase attention to critical input tokens or decrease
761 attention to less informative tokens. Lu et al. (2021) proposes a mask perturbation method to ad-
762 just attention weights for key tokens, thereby improving translation quality. Zhang et al. (2023a)
763 introduce PASTA, which allows manual designation of important tokens during inference. This is
764 extended by AutoPASTA (Zhang et al., 2024a), which uses LLMs to autonomously identify salient
765 tokens and increase attention to them. In contrast, ACT (Yu et al., 2024) reduces attention to se-
766 mantic trivial sink tokens and redirects it to meaningful content. Similar strategies have been applied
767 to VLMs to mitigate hallucinations. PAI (Liu et al., 2024b) enhances attention to image tokens at
768 inference time to counteract text-dominant bias. IBD (Zhu et al., 2024) and OPERA (Wei & Zhang,
769 2024) further refine this idea by prioritizing visual information or penalizing overconfident summary
770 tokens. While effective, these methods depend on identifying task-specific tokens, which may intro-
771 duce bias (e.g., overemphasizing misleading tokens) and limit applicability when token importance
772 is unclear or attention maps are unavailable. In contrast, our method focuses on a task-invariant
773 initial token, removing the need for costly token identification, and can be easily applied by tuning
774 key states.

775 A.2 THE MAGIC OF THE INITIAL TOKEN
776

777 Recent studies highlight the significance of the initial token, especially through the lens of the *at-*
778 *tention sink* phenomenon, where it draws substantial attention despite low semantic content. Xiao
779 et al. (2023) show that preserving such tokens is critical for maintaining performance in sliding win-
780 dows attention. Kaul et al. (2024) attribute this effect to softmax normalization and causal masking,
781 while Gu et al. (2024) and Barbero et al. (2025) identify architectural biases that amplify attention
782 to the initial token, including key-query alignment and LayerNorm effects. Functionally, the initial
783 token is hypothesized to serve as a stabilizing “no-op” anchor, enhancing robustness to prompt
784 variations (Barbero et al., 2025). It has been leveraged in applications such as long-context mod-
785 eling (Zhang et al., 2023b; Xiao et al., 2023), but also poses challenges for quantization due to its
786 high attention weight (Dettmers et al., 2023; Liu et al., 2024a). While previous work has identified
787 the structural and functional importance of the initial token, its potential as a target for attention
788 tuning remains underexplored. In this work, we provide a detailed analysis of attention tuning of the
789 initial token across layers and heads, demonstrating its consistent influence across different tasks.
790 Our approach bridges the gap between the these lines of research by proposing a novel method that
791 advances interpretable attention tuning.

792 B DETAILED EXPERIMENTAL SETUP
793

794 **Models, Tasks, and Datasets.** Models: We evaluate ZeroTuning on four LLMs with distinct at-
795 tention implementations: Llama-3.1-8B-Instruct (Grattafiori et al., 2024) and Llama-2-13B-Chat
796 (Touvron et al., 2023) with eager attention, Qwen-2-7B (Yang et al., 2024) with SDPA attention,
797 and DeepSeek-R1-14B (DeepSeek-AI et al., 2025) with Flash attention.² Tasks and Datasets: Our
798 experiments encompass three task types across 15 datasets: (1) Text Classification and Reasoning,
799 including SST-2 (binary sentiment classification) (Socher et al., 2013), SST-5 (fine-grained senti-
800 ment analysis) (Socher et al., 2013), MR (movie review polarity detection) (Pang & Lee, 2005),
801 SUBJ (subjectivity classification) (Pang & Lee, 2004), TREC (question type classification) (Li &
802 Roth, 2002), CB (commitment detection) (De Marneffe et al., 2019), and BoolQ (boolean question
803 answering) (Clark et al., 2019); (2) Domain-Specific Multiple-Choice, including MMLU (cross-
804 domain knowledge testing) (Hendrycks et al., 2020), AQUA (math word problems) (Zheng et al.,
805 2024a), MathQA (algebraic reasoning) (Amini et al., 2019), LogiQA (logical reasoning) (Liu et al.,
806 2023), CQA (commonsense reasoning) (Talmor et al., 2018), PIQA (physical commonsense QA)
807 (Bisk et al., 2020), and ARCC (scientific reasoning) (Clark et al., 2018); and (3) Multi-Round Con-
808 versation, using MT-Bench (Zheng et al., 2024a).

809 ²Eager, SDPA, and Flash are official attention implementations in modern Transformer libraries. Eager
810 computes the full attention map; SDPA uses PyTorch’s efficient API to select the optimal implementation;
811 Flash relies on fused CUDA kernels from the FlashAttention library.

Baselines and Evaluation Metrics. Baselines: We benchmark ZeroTuning against three baselines: (1) vanilla inference, which performs standard inference without any modifications; (2) ACT (Yu et al., 2024), which identifies non-initial sink tokens using an attention score threshold and reduces their attention weights; and (3) Auto-PASTA (Zhang et al., 2024a), which leverages an LLM to locate important tokens and enhance their attention weights. Evaluation Metrics: We assess performance using accuracy for text classification and multiple-choice tasks. For the multi-round conversation task, we report average quality scores as evaluated by GPT-4, following the methodology outlined in Zheng et al. (2024a).

Implementation Details. All experiments are implemented in PyTorch using the Hugging Face Transformers library. We use a zero-shot setting with greedy decoding for consistency across all methods. For our supervised variant and the baselines, we use a fixed validation set of 500 randomly selected samples (seed 42) for calibration. For ZeroTuning, we tune the top 40% of identified heads unless otherwise specified. For ACT, we use the official hyperparameter ($\beta = 0.4$), and since it requires explicit attention maps, we only evaluate it on Llama-3.1-8B-Instruct. Prompts for all tasks and baselines are detailed in Appendix O.

C THEORETICAL ANALYSIS OF TUNING EFFICACY VIA THE INITIAL TOKEN

This appendix provides a formal proof for the claim made in Section 3.1: that the tuning effect’s magnitude is governed by the initial token’s attention weight a_0 .

Proposition 1. *For any given scaling factor $\gamma \neq 1$ and any two non-initial tokens $i, j \geq 1$ with unequal initial attention weights ($a_i \neq a_j$), the magnitude of the tuning effect on their attention difference is a strictly monotonically increasing function of the initial token’s attention weight, a_0 .*

We aim to show that the tuning effect, $E_{\text{diff},i,j}$, is a monotonically increasing function of a_0 by proving its partial derivative with respect to a_0 is positive. Recall the definition of the effect magnitude from Eq. equation 5:

$$E_{\text{diff},i,j}(a_0) = |a_i - a_j| \frac{|\gamma - 1| a_0}{(\gamma - 1) a_0 + 1}. \quad (7)$$

Taking the partial derivative of E_{diff} with respect to a_0 , we treat the term $|a_i - a_j| |\gamma - 1|$ as a constant factor:

$$\frac{\partial E_{\text{diff},i,j}}{\partial a_0} = |a_i - a_j| |\gamma - 1| \cdot \frac{\partial}{\partial a_0} \left(\frac{a_0}{(\gamma - 1) a_0 + 1} \right) \quad (8)$$

$$= |a_i - a_j| |\gamma - 1| \cdot \frac{1 \cdot ((\gamma - 1) a_0 + 1) - a_0 \cdot (\gamma - 1)}{((\gamma - 1) a_0 + 1)^2} \quad (9)$$

$$= |a_i - a_j| |\gamma - 1| \cdot \frac{1}{((\gamma - 1) a_0 + 1)^2}. \quad (10)$$

The term $|a_i - a_j| |\gamma - 1|$ is non-negative. The denominator, $((\gamma - 1) a_0 + 1)^2 = D^2$, is the square of the normalization constant and is strictly positive for any valid probability distribution. Therefore, the derivative $\frac{\partial E_{\text{diff},i,j}}{\partial a_0} \geq 0$.

Furthermore, for any non-trivial case where the tuning factor is active ($\gamma \neq 1$) and the attention weights are not uniform ($a_i \neq a_j$ for some i, j), the derivative is strictly positive. This proves that E_{diff} is a strictly monotonically increasing function of a_0 . Consequently, a larger initial attention weight provides a more powerful lever for modulating the attention distribution. This theoretical result is visually corroborated by Figure 9.

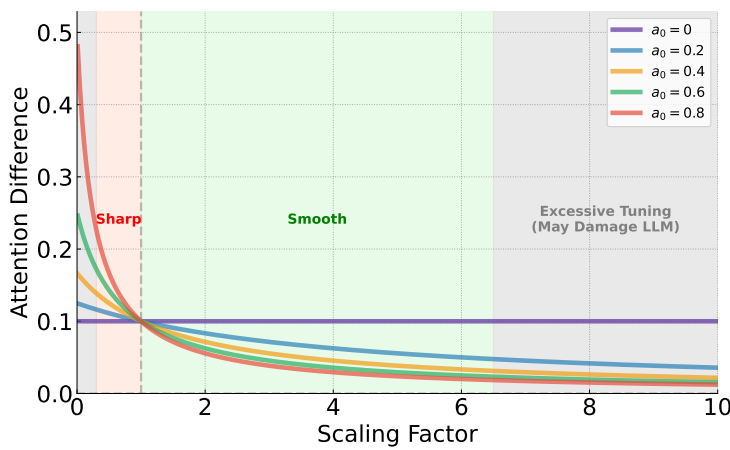


Figure 9: Visualization of the tuning effect on attention differences $|a'_i - a'_j|$ as a function of the scaling factor γ for various initial attention weights $a_0 \in \{0, 0.2, 0.4, 0.6, 0.8\}$. The plot demonstrates that a higher initial attention weight a_0 (e.g., the red curve) leads to a significantly stronger response to changes in γ . We identify three primary regimes: **sharpening** ($\gamma < 1$), where attention differences are amplified; **smoothing** ($\gamma > 1$), where differences are diminished; and regions of **excessive tuning** (e.g., $\gamma \rightarrow 0$ or $\gamma \gg 1$), which may degrade performance.

D DEEPER ANALYSIS OF POTENTIAL FAILURES AND NEGATIVE EFFECTS

To provide a comprehensive understanding of ZeroTuning, we analyze its operational boundaries and potential negative side effects when pushed to its limits.

Boundaries of Efficacy: Unlocking Latent Knowledge vs. Correcting Factual Errors. Our analysis reveals a key insight into ZeroTuning’s mechanism: it primarily unlocks and disambiguates a model’s latent knowledge, rather than correcting deeply ingrained factual errors. To test this, we quantitatively analyzed ZeroTuning’s corrective power as a function of the vanilla model’s initial prediction confidence. We partitioned the set of SST2 incorrect predictions into “uncertain errors” (vanilla softmax confidence $<$ threshold) and “certain errors” (confidence \geq threshold) and evaluated our method’s performance on each group.

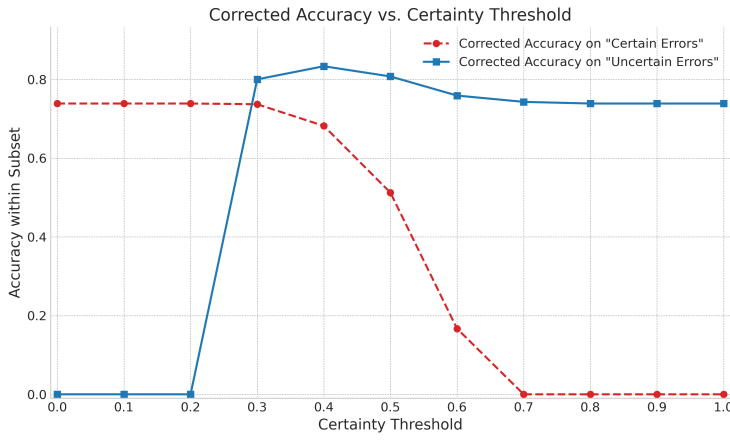


Figure 10: Corrected accuracy on initially incorrect samples as a function of the vanilla model’s confidence (certainty threshold).

The results, shown in Figure 10, provide strong empirical validation. ZeroTuning is highly effective on the uncertain error population (blue line), correcting over 80% of mistakes where the vanilla

918 model’s confidence was below 0.5. Conversely, its ability to fix certain errors (red line) decays
 919 sharply as the base model’s confidence increases, dropping to near-zero on predictions where the
 920 model was already confidently wrong. This confirms a clear operational boundary: ZeroTuning
 921 excels at resolving low-confidence mistakes by refining the model’s focus, but it is not designed to
 922 overwrite high-confidence knowledge learned during pretraining.

923 This finding positions ZeroTuning not as a replacement for fine-tuning, but as a powerful, com-
 924plementary inference-time technique. It assists a model in better leveraging its existing, albeit
 925 sometimes uncertain, knowledge. The potential for synergistic interaction between ZeroTuning and
 926 parameter-efficient fine-tuning methods like LoRA remains a promising avenue for future research.
 927

928 **Negative Effects of Extreme Tuning.** We also investigated the effects of applying extreme scaling
 929 factors (γ), far outside the optimal range. These experiments reveal predictable failure modes that
 930 further illuminate the role of the initial token:

- 931 • **Overly-suppressed attention** ($\gamma \rightarrow 0$): When the initial token’s attention is excessively
 932 reduced, the model’s output often becomes degenerative. We observe a tendency for the
 933 model to enter repetitive loops, outputting a single answer (e.g., “True”) without any of
 934 the semantic elaboration or reasoning present in the vanilla output. This suggests that a
 935 minimal level of attention to the “sink” token is necessary to maintain generative stability.
 936
- 937 • **Overly-amplified attention** ($\gamma \gg 1$): Conversely, when the initial token’s attention is
 938 excessively high, it can disrupt the model’s ability to follow complex instructions. By
 939 absorbing too much of the attention budget, the initial token appears to prevent other, more
 940 task-relevant tokens from receiving the focus they need, leading to incomplete or non-
 941 compliant answers.

942 Interestingly, within a reasonable range, moderate tuning of the initial token’s attention can produce
 943 effects analogous to adjusting the temperature parameter in decoding. It can modulate the diver-
 944 sity of the output, encouraging the model to explore different perspectives or generate more varied
 945 responses, without the repetitive downsides of extreme scaling.

946 However, our method is fundamentally more powerful for error correction. Temperature scaling
 947 acts on the final logits z just before the softmax, calculating the probability of the i -th token as
 948 $p_i = \text{softmax}(z_i/T)$. Since dividing by a positive temperature T does not change the relative order
 949 of the logits (i.e., $\arg \max_i(z_i) = \arg \max_i(z_i/T)$), temperature scaling cannot alter the outcome
 950 of greedy decoding. In contrast, ZeroTuning operates at the attention level, optimizing the model’s
 951 internal representations. This process produces an entirely new set of output logits, z' , which can
 952 have a different rank ordering. It is therefore possible for the originally predicted token $\arg \max_i(z_i)$
 953 to be incorrect, while the new prediction $\arg \max_i(z'_i)$ becomes correct, enabling error correction.

954 E UNSUPERVISED ZEROTUNING: ANALYSIS AND RESULTS

955 This section details the unsupervised variant of ZeroTuning, which eliminates the need for a labeled
 956 calibration set by leveraging the model’s output entropy as a proxy for performance.

957 We begin with a visual analysis to establish the core principle behind this approach. Figure 11
 958 plots three key metrics against the attention scaling factor γ : the average next-token entropy, its
 959 logarithm, and the final task accuracy. The plots reveal a compelling and consistent pattern across
 960 all datasets. The average entropy curve (left subplot) exhibits a distinct U-shape, identifying a
 961 clear scaling factor that minimizes the model’s predictive uncertainty. Critically, the trough of these
 962 entropy curves aligns remarkably well with the peak, or a near-peak plateau, in the accuracy curve
 963 (right). This strong visual correlation provides powerful evidence that minimizing entropy can serve
 964 as a robust, unsupervised signal for identifying a high-performance region for γ .

965 Guided by this insight, we quantify the effectiveness of an unsupervised approach where we select
 966 the γ that minimizes entropy on the unlabeled test set. Table 4 compares its performance against the
 967 vanilla baseline and the supervised ZeroTuning variant. The results demonstrate that the unsuper-
 968 vised method is remarkably effective, achieving an average score of 67.02—highly competitive with
 969 the supervised result of 67.52 and a substantial improvement over the vanilla baseline’s 59.00. No-
 970 tably, on LogiQA, the entropy-guided method even slightly outperforms its supervised counterpart.
 971

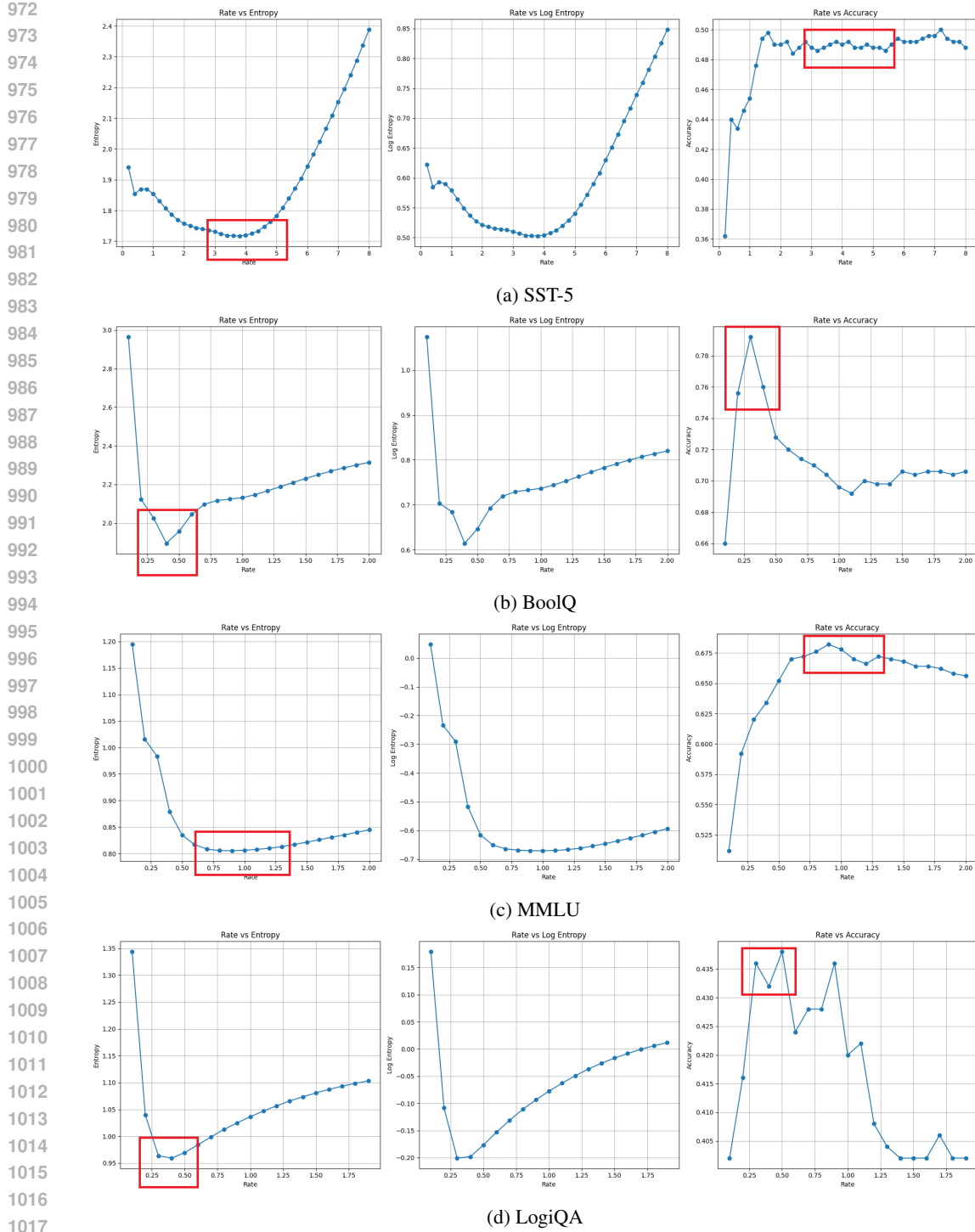


Figure 11: Visualizing the relationship between the scaling factor γ and three key metrics: average entropy (left), log-entropy (middle), and task accuracy (right). Across diverse datasets, the entropy minimum consistently aligns with a region of high accuracy, validating entropy as a strong signal for unsupervised tuning.

This quantitative validation confirms that unsupervised ZeroTuning is a powerful and practical alternative, transforming our method into a versatile tool that can be deployed without any task-specific labeled data.

1026 Table 4: Performance comparison of Vanilla, Supervised, and Unsupervised ZeroTuning on Llama-
 1027 3.1-8B-Instruct. The best performance in each column is **bolded**.

1028

| 1029 Method | 1030 SST-2 | 1031 SST-5 | 1032 BoolQ | 1033 MMLU | 1034 LogiQA | 1035 Avg. |
|--------------------------------|-------------------|-------------------|-------------------|------------|-------------------|-------------------|
| 1031 Vanilla | 1032 73.20 | 1033 45.40 | 1034 69.60 | 1035 67.40 | 1036 39.40 | 1037 59.00 |
| 1032 ZeroTuning (Supervised) | 1033 91.60 | 1034 52.00 | 1035 82.40 | 1036 68.80 | 1037 42.80 | 1038 67.52 |
| 1033 ZeroTuning (Unsupervised) | 1034 90.20 | 1035 51.80 | 1036 80.80 | 1037 68.80 | 1038 43.50 | 1039 67.02 |

1034

1035

E.1 DEEPER ERROR ANALYSIS FOR UNSUPERVISED ZEROTUNING

1037

1038

A key finding of our analysis is that while minimizing entropy on individual samples can be misleading, minimizing the *average* entropy across a dataset robustly identifies an optimal tuning parameter. This suggests Unsupervised ZeroTuning corrects for systemic, dataset-level biases rather than isolated prediction errors. To understand this phenomenon, we analyze how the method behaves on different error types for SST2.

1042

1043

The Unreliable Entropy Landscape of Uncertain Samples. We first examine "uncertain" samples, where the vanilla model's confidence in its top-choice token is low (e.g., $p_{top} < 0.5$). For these samples, the entropy landscape is often deceptive and contains two primary "traps":

1046

1047

1048

1049

1050

1051

1052

1053

1054

1055

1056

1057

1058

1059

1060

1061

1062

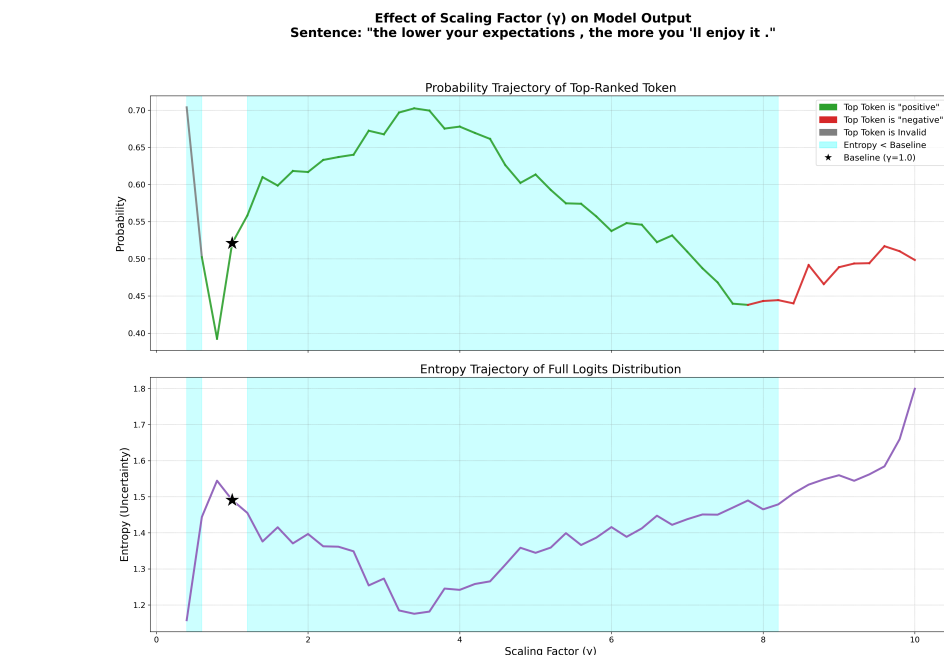
1063

1064

1065

1066

1067



1068

1069

1070

1071

Figure 12: An uncertain sample where the correct answer is "negative". The vanilla model incorrectly outputs "positive". For $\gamma < 1$, the model outputs an invalid format. For $\gamma > 1$, it first amplifies the probability of the initial incorrect answer before flipping to the correct one. The entropy minima are misleadingly located in the regions of the invalid and incorrect answers.

1072

1073

1074

1075

1076

1077

1078

1079

1. **The Format Trap ($\gamma < 1$):** When reducing the initial token's attention, the model enters a "local-focused" mode. For uncertain samples, this can amplify attention on unintended tokens, leading to a violation of task instructions. In this mode, the model often outputs tokens outside the constrained answer space, such as "neutral" or "The", instead of the required "positive" or "negative". As γ decreases below 1, the model's confidence in this wrongly formatted token can increase, creating a misleading drop in entropy.
2. **The Bias Amplification Trap ($\gamma > 1$):** When increasing the initial token's attention, the model enters a "global-integrative" mode. For an initially incorrect, uncertain sample, this

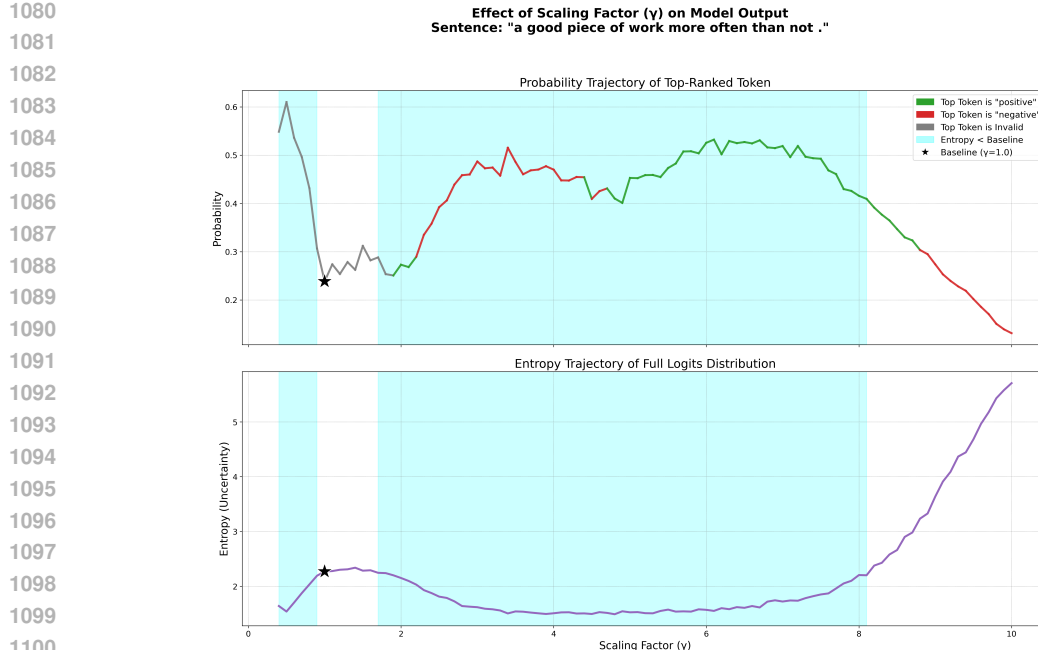
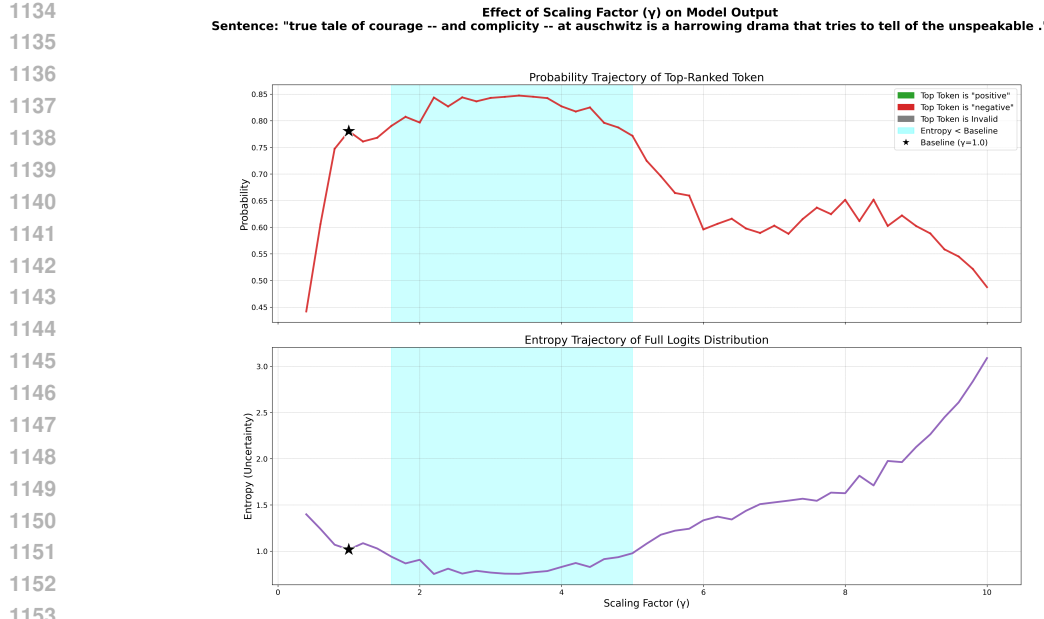


Figure 13: A more uncertain sample where the correct answer is "positive". The vanilla model incorrectly outputs "neutral" (an invalid format). As γ increases, the model first transitions to a valid but incorrect answer ("negative") before finally flipping to the correct answer ("positive"). The entropy landscape exhibits multiple local minima corresponding to the invalid, incorrect, and correct answers, making direct judgment based on the global minimum unreliable.

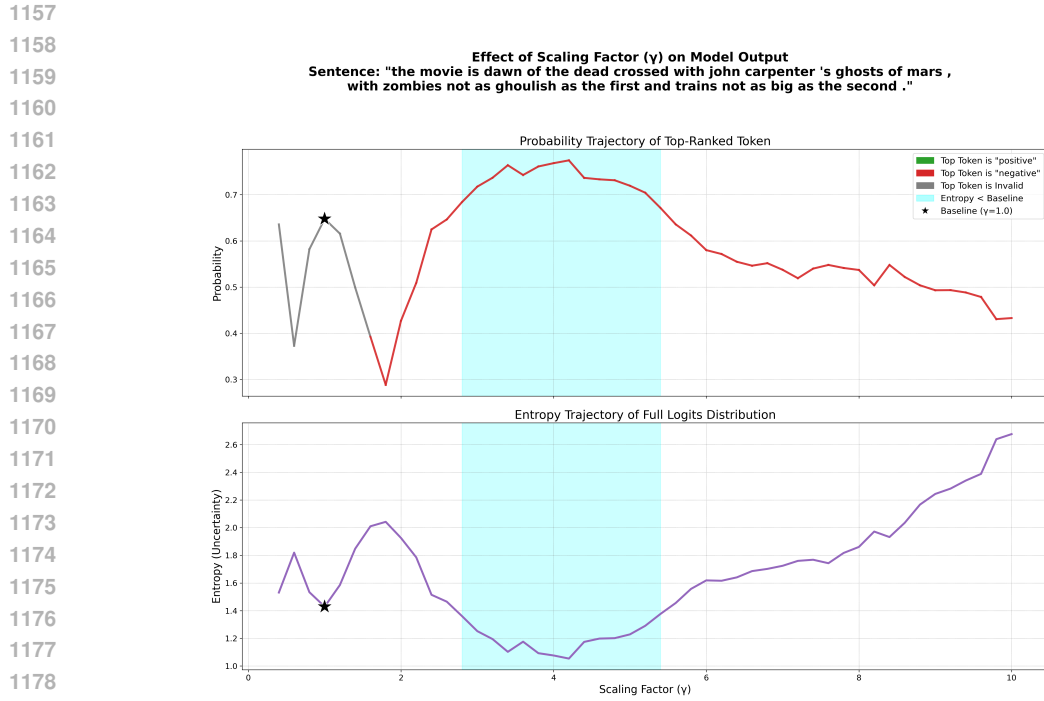
often induces a "competing peaks" phenomenon. Both Figure 12 and 13 illustrate cases where the model first amplifies an existing bias, leading to a deep entropy well corresponding to an incorrect answer. Only with further increases in α does the model's interpretation "flip" to the correct one. Figure 13 shows a more complex cascade: after overcoming the format trap, the model first falls into a bias trap (incorrectly predicting "negative" due to the word "not") before finally settling on the correct answer ("positive"). In both cases, if the global entropy minimum is sought, it may lock onto an amplified bias or a formatting error, creating a trap.

The Stabilizing Behavior of Certain Samples. In contrast, "certain" samples (where $p_{top} \geq 0.5$) exhibit more predictable behavior and act as a stabilizing force during average entropy minimization. We identify two sub-types:

- **Recalcitrant Certain Errors:** As shown in Figure 14, if the model is confidently wrong but its answer is *within the valid format* (e.g., predicting "negative" for a positive sentence), its semantic conviction is strong. In this case, modulating γ reinforces this conviction, leading to a stable, uni-modal probability peak. The error is not corrected. This suggests the model's relevant pretrained knowledge is already strongly activated, albeit towards an incorrect conclusion. These samples act as a stable "ballast" in the collective average.
- **Correctable Certain Errors:** As shown in Figure 15, if the model is confidently wrong because it produced an *out-of-format* token (e.g., "neutral"), the error is rooted in a misunderstanding of task constraints/instruction, not deep semantic conviction. Here, the model's pretrained knowledge is "locked". Modulating γ (specifically, increasing it) helps the model refocus on the instructions, "unlocking" its latent knowledge and guiding it to the correct, in-format answer. In these cases, the entropy minimum correctly corresponds to the right answer.

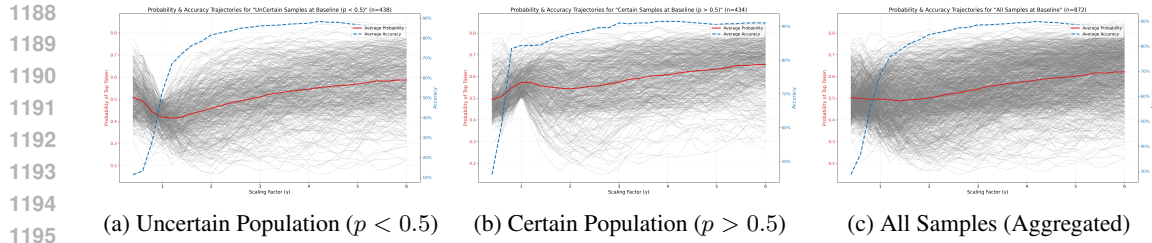


1154 Figure 14: A **recalcitrant** certain sample. The vanilla model (*) predicts an incorrect but in-format
1155 answer ("negative") with high confidence. Modulating γ only reinforces this conviction without an
1156 answer flip.



1180 Figure 15: A **correctable** certain sample. The vanilla model (*) predicts an out-of-format answer
1181 ("neutral") with high confidence. Increasing α guides the model to overcome the format error and
1182 output the correct answer ("negative").

1183
1184
1185 **Why Collective Signal Works Better?** The visualizations in Figure 16 reveal a key insight:
1186 while individual uncertain samples exhibit highly irregular and sometimes multi-peaked probabili-
1187 ty/accuracy trajectories as γ varies, the aggregate signal constructed from many samples becomes
1188 smooth, stable, and strongly aligned with true accuracy improvement.



1196 Figure 16: Population-level probability and accuracy trajectories. Gray lines represent individual
1197 samples. Red: average probability of the top token. Blue: average accuracy.

1200 We observe two complementary mechanisms:

- 1202 • **Statistical Cancellation for $\gamma < 1$.** Uncertain samples tend to fall into the format trap and
1203 display artificially low entropy for invalid outputs, whereas certain samples consistently
1204 lose confidence when γ decreases. When averaged, these opposing trends cancel out, pro-
1205 ducing a flat and stable population-level curve. This prevents the collective entropy signal
1206 from being dominated by pathological samples.
- 1207 • **Signal Reinforcement for $\gamma > 1$.** In this region, both populations—despite their very
1208 different behaviors at the individual level—exhibit a shared upward trend in accuracy as γ
1209 increases. This alignment creates a resonant effect: the aggregated probability and accuracy
1210 curves become smoother and strongly monotonic, reliably pointing toward the globally
1211 beneficial regime of $\gamma > 1$.

1212 Together, these effects explain why Unsupervised ZeroTuning succeeds when optimizing the aver-
1213 age entropy. The population average filters out idiosyncratic traps (format errors, bias amplifica-
1214 tions) and amplifies the underlying structural signal that reflects the model’s latent reasoning and
1215 instruction-following capabilities. This makes the minimum of the average-entropy curve over γ a
1216 trustworthy indicator of the optimal tuning direction.

1218 F LLM OUTPUT EXAMPLE

1220 F.1 EXAMPLES OF SST-2 DATASET

1223 Example 1:

1224 Classify the sentence into one of the following sentiments: positive or negative.
1225 Sentence: “hardly a masterpiece, but it introduces viewers to a good charitable
1226 enterprise and some interesting real people.”

1227 Sentiment:

1228 **Vanilla Output:** negative. Explanation: The sentence describes the movie as
1229 “hardly a masterpiece”, which is a negative description. The positive aspects men-
1230 tioned in the sentence are secondary to the negative description. Therefore, the
1231 overall sentiment of the sentence is negative.

1232 **ZeroTuning Output ($\gamma = 4$):** positive. Explanation: The word “good” in the
1233 sentence has a positive connotation, and the word “interesting” also has a positive
1234 connotation. This indicates that the overall sentiment of the sentence is positive.
1235 The word “hardly” is a negative word, but in this context, it is used to express
1236 a mild criticism, so it does not dominate the overall sentiment of the sentence.
1237 Therefore, the sentence is classified as having a positive sentiment.

1238 **Ground Truth:** positive

1239 Example 2:

1240 Classify the sentence into one of the following sentiments: positive or negative.
1241 Sentence: “generally, clockstoppers will fulfill your wildest fantasies about being

1242 a different kind of time traveler, while happily killing 94 minutes.”
 1243 Sentiment:
 1244 **Vanilla Output:** negative. Explanation: Although the sentence mentions “wildest
 1245 fantasies,” which can be interpreted as positive, the overall tone is negative due
 1246 to the phrase “happily killing 94 minutes.” This phrase implies that the movie is
 1247 a waste of time and that the viewer will lose 94 minutes of their life watching
 1248 it. This negative connotation outweighs the potential positive interpretation of
 1249 “wildest fantasies,” leading to a classification as a negative sentiment.
 1250 **ZeroTuning Output** ($\gamma = 4$): positive. Reasoning skill: Emotion Recognition
 1251 And Sentiment Analysis. The sentence is classified as positive because it uses
 1252 words with positive connotations such as “wildest fantasies” and “happily”, which
 1253 suggest a sense of excitement and enjoyment. The phrase “fulfill your wildest
 1254 fantasies” implies that the experience of being a clockstopper is desirable and
 1255 thrilling. Additionally, the word “happily” reinforces this positive sentiment.
 1256 **Ground Truth:** positive

1257 **Example 3:**

1258 Classify the sentence into one of the following sentiments: positive or negative.
 1259 Sentence: “whether you like rap music or loathe it, you can’t deny either the
 1260 tragic loss of two young men in the prime of their talent or the power of this
 1261 movie.”
 1262 Sentiment:
 1263
 1264 **Vanilla Output:** neutral. The sentiment of this sentence is neutral because it
 1265 neither praises nor criticizes rap music, but rather acknowledges its impact on
 1266 society. The sentence also expresses a sense of sadness and loss, but in a factual
 1267 and matter-of-fact way, rather than with strong emotion. The word “tragic” is a
 1268 strong word, but it is used to describe a fact, rather than to express a personal
 1269 opinion or feeling. Overall, the tone of the sentence is informative and objective,
 1270 rather than emotional or biased
 1271 **ZeroTuning Output** ($\gamma = 2$): positive. Reasoning Skill: This question requires
 1272 the ability to identify the sentiment of a sentence, which is a fundamental skill in
 1273 Emotion Recognition and Sentiment Analysis. The sentence presents a neutral
 1274 statement about rap music, but the overall tone is positive due to the mention
 1275 of the “tragic loss” and the “power” of the movie, which suggests a sense of
 1276 admiration and respect. The correct answer requires the reader to analyze the
 1277 sentence and recognize the underlying sentiment, and classify the sentence as
 1278 positive or negative.
 1279 **Ground Truth:** positive

1280
 1281 F.2 EXAMPLES OF BOOLQ DATASET

1282 **Example 1:**

1283 Read the text and answer the question by True or False.
 1284 Text: Hawaii Five-0 (2010 TV series, season 8) – The eighth season of the CBS
 1285 police procedural drama series Hawaii Five-0 premiered on September 29, 2017
 1286 for the 2017–18 television season. CBS renewed the series for a 23 episode eighth
 1287 season on March 23, 2017. However, on November 6, 2017 CBS ordered an
 1288 additional episode for the season and did the same again on February 8, 2018
 1289 bringing the count to 25 episodes. The season concluded on May 18, 2018. The
 1290 eighth season ranked #18 for the 2017-18 television season and had an average of
 1291 11 million viewers. The series was also renewed for a ninth season.
 1292 Question: will hawaii five o have a season 8?
 1293 Answer:
 1294 **Vanilla Output:** False. The text says the series has already concluded its 8th
 1295 season. (Note: this question is not about whether the series will be renewed for

1296
1297
1298

a 9th season, but whether it will have an 8th season, which it has already done). (Note: the series was renewed for a 9th season, but that is not relevant to the question).

1299
1300
1301
1302
1303
1304
1305

ZeroTuning Output ($\gamma = 0.3$): True. (It is already confirmed by CBS). The season premiered on September 29, 2017 and concluded on May 18, 2018. It was renewed for a 23 episode eighth season on March 23, 2017 and had 25 episodes in total. (The extra two episodes were ordered on November 6, 2017 and February 8, 2018). The series also ranked 18 for the 2017-18 television season and had an average of 11 million viewers.

Ground Truth: True

1306
1307

Example 2:

1308
1309
1310
1311
1312
1313

Read the text and answer the question by True or False.

Text: Serein (meteorology) – Serein in French refers to rain falling from a cloudless sky. This sort of rain is said to take on the form of a fine, light drizzle, typically after dusk. The name derives from French serein, meaning “serene”, or “clear” (as in unclouded). An alternative etymology is from Old French serain, evening.

Question: can it rain if there are no clouds?

1314
1315
1316
1317
1318
1319
1320
1321

Answer:

Vanilla Output: False, Serein is rain falling from a cloudless sky. Therefore, there are clouds, but they are not visible. Serein is not rain falling from a completely clear sky. Therefore, it is not possible for it to rain if there are no clouds.

ZeroTuning Output ($\gamma = 0.3$): True. (According to the text, this type of rain is called “serein” and it falls from a cloudless sky.) False. (This is a common misconception, but it’s not true that it can’t rain if there are no clouds.) (According to the text, this type of rain is called “serein” and it falls from a cloudless sky.)

Ground Truth: True

1322
1323
1324

G THE EFFECT OF TUNING DIFFERENT MATRICES

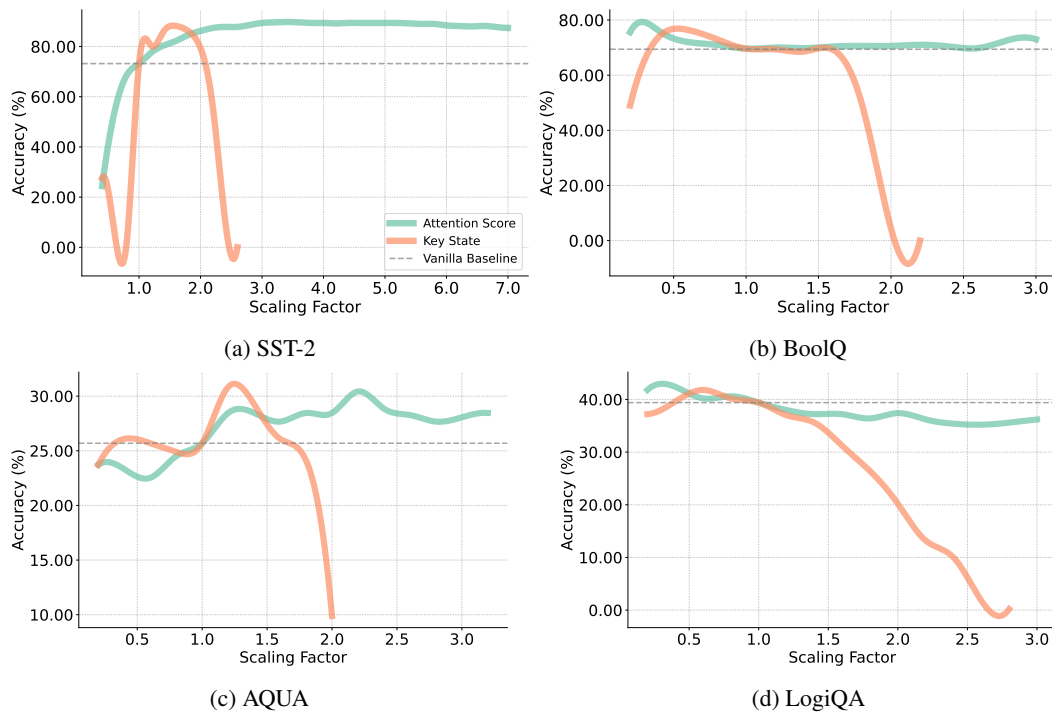


Figure 17: Accuracy of tuning the initial token’s attention scores and key states over (a) SST-2, (b) BoolQ, (c) AQUA, and (d) LogiQA.

1347
1348
1349

1350 In certain scenarios where the attention map is not explicitly computed, it is challenging to influence
 1351 the final representation by modifying the attention weights. Therefore, we consider tuning the key
 1352 or query states as an alternative approach. As illustrated in the Figure 17, we observe that within an
 1353 appropriate scaling range, tuning the key state exhibits a similar trend to tuning the attention score.
 1354 However, we find that directly tuning the key states is more sensitive: when the scaling factor is
 1355 too small or too large, the performance of the LLM drops sharply, while tuning the attention score
 1356 results in more stable performance.

1357 We now analyze the theoretical differences between applying the scaling factor γ to the attention
 1358 scores versus the key states. To begin, we revisit and extend the attention weight formulation from
 1359 Section 3.1. For a sequence of length T , the attention weight for token i is given by:
 1360

$$1361 \quad 1362 \quad a_i = \frac{\exp(z_i)}{\sum_{m=0}^{T-1} \exp(z_m)}, \quad 1363$$

1364 where z_i denotes the logit for token i , given by:
 1365

$$1366 \quad 1367 \quad z_i = \frac{\mathbf{q}^\top \mathbf{k}_i}{\sqrt{d_k}}, \quad 1368$$

1370 with $\mathbf{q} \in \mathbb{R}^{d_k}$ as the query vector, $\mathbf{k}_i \in \mathbb{R}^{d_k}$ as the key vector for token i , and d_k as the dimension-
 1371 ality of the key vectors. Note that a_0 corresponds to the initial token, and $\sum_{i=0}^{T-1} a_i = 1$.
 1372

1373 **Tuning the Attention Score** As derived in Section 3.1, when tuning the attention score, the dif-
 1374 ference between the attention weights of non-initial tokens $i, j \geq 1$ becomes:
 1375

$$1376 \quad 1377 \quad a'_i - a'_j = \frac{a_i - a_j}{D} = \frac{a_i - a_j}{(\gamma - 1)a_0 + 1}. \quad 1378$$

1379 Next, we expand a_0 , a_i , and a_j as follows:
 1380

$$1381 \quad 1382 \quad a'_i - a'_j = \frac{a_i - a_j}{(\gamma - 1)a_0 + 1} \\ 1383 \quad 1384 \quad = \frac{\exp(z_i) - \exp(z_j)}{\left(\sum_{k=0}^{T-1} \exp(z_k) \right) \left[(\gamma - 1) \frac{\exp(z_0)}{\sum_{k=0}^{T-1} \exp(z_k)} + 1 \right]} \\ 1385 \quad 1386 \quad = \frac{\exp(z_i) - \exp(z_j)}{(\gamma - 1) \exp(z_0) + \sum_{k=0}^{T-1} \exp(z_k)}. \quad 1387$$

1390 **Tuning the Key State** Now, consider scaling the key state by γ , i.e., $\mathbf{k}'_0 = \gamma \mathbf{k}_0$. This changes the
 1391 logit for the initial token:
 1392

$$1393 \quad 1394 \quad z'_0 = \frac{\mathbf{q}^\top (\gamma \mathbf{k}_0)}{\sqrt{d_k}} = \gamma z_0, \quad 1395$$

1397 while the logits for other tokens remain unchanged: $z'_i = z_i$ for $i \geq 1$. The tuned attention weights
 1398 are then:
 1399

$$1400 \quad 1401 \quad a'_i = \frac{\exp(z'_i)}{\sum_{j=0}^{T-1} \exp(z'_j)} = \frac{\exp(z_i)}{\exp(\gamma z_0) + \sum_{j=1}^{T-1} \exp(z_j)}, \quad \text{for } i \geq 1. \quad 1402$$

1403 The attention difference for non-initial tokens $i, j \geq 1$ is derived as:

$$\begin{aligned}
a'_i - a'_j &= \frac{\exp(z_i)}{\exp(\gamma z_0) + \sum_{k=1}^{T-1} \exp(z_k)} - \frac{\exp(z_j)}{\exp(\gamma z_0) + \sum_{k=1}^{T-1} \exp(z_k)} \\
&= \frac{\exp(z_i) - \exp(z_j)}{\exp(\gamma z_0) + \sum_{k=1}^{T-1} \exp(z_k)}. \tag{17}
\end{aligned}$$

The denominator in equation 14 includes the linear term $(\gamma - 1) \exp(z_0)$ of γ , whereas the denominator in equation 17 contains the exponential component $\exp(\gamma z_0)$. This indicates that tuning the attention weights results in a smoother effect, while tuning the key states has a more abrupt impact.

Beyond the effect on attention differences, we can analyze the final representations to understand the stability disparity. The final representation \mathbf{o}' is a weighted sum of value vectors, $\mathbf{o}' = \sum a'_i \mathbf{v}_i$. The structure of these weights a'_i dictates the stability of \mathbf{o}' .

Representation from Tuning Attention Scores. The output representation is a convex combination of value vectors, as the normalized weights a'_i sum to one. Specifically:

$$\mathbf{o}'_{\text{attn}} = \left(\frac{\gamma a_0}{(\gamma - 1)a_0 + 1} \right) \mathbf{v}_0 + \sum_{i=1}^{T-1} \left(\frac{a_i}{(\gamma - 1)a_0 + 1} \right) \mathbf{v}_i. \tag{18}$$

Crucially, the coefficients of \mathbf{v}_i are smooth rational functions of γ . This ensures that the output representation $\mathbf{o}'_{\text{attn}}$ changes smoothly and its magnitude remains bounded by the magnitudes of the value vectors. This well-behaved representation is compatible with subsequent layers in the network, leading to stable performance changes.

Representation from Tuning Key & Query States. This method also produces a convex combination. However, its stability is undermined by the exponential nature of the weights:

$$\mathbf{o}'_{\text{key}} = \left(\frac{\exp(\gamma z_0)}{Z'} \right) \mathbf{v}_0 + \sum_{i=1}^{T-1} \left(\frac{\exp(z_i)}{Z'} \right) \mathbf{v}_i, \quad \text{where } Z' = \exp(\gamma z_0) + \sum_{j=1}^{T-1} \exp(z_j). \tag{19}$$

The instability arises from the exponential sensitivity of the leading coefficient to the scaling factor γ . Due to the $\exp(\gamma z_0)$ term, the weight applied to \mathbf{v}_0 grows exponentially with γ . For large values of γ , this exponential amplification causes the initial token’s attention weight to rapidly saturate towards 1, forcing the weights of all other tokens towards 0. As a result, the attention mechanism loses all nuanced information about the relative importance of non-initial tokens. The output \mathbf{o}'_{key} ceases to be a meaningful synthesis of context, instead collapsing to approximately \mathbf{v}_0 .

Even though the magnitude of \mathbf{o}'_{key} is bounded, the information-impoverished representation fed to subsequent layers cripples the model’s reasoning ability, causing the observed sharp drop in accuracy.

H PERFORMANCE UNDER RESOURCE CONSTRAINTS

Computational constraints are common in real-world applications and can limit the feasibility of head classification and parameter optimization in LLMs. To investigate how well ZeroTuning adapts to such conditions, we define three resource constraint levels based on available computational resources:

- **Level 0:** Severely limited resources that prevent both head classification and parameter search.
- **Level 1:** Moderately limited resources that allow parameter search but not head classification.
- **Level 2:** Ample resources that support both head classification and parameter search.

We evaluate ZeroTuning’s performance across these levels using the LLaMA-3.1-8B model. At Level 0, we apply fixed scaling factors ($\gamma = 2$ and $\gamma = 0.6$) to all attention heads, reflecting

dataset-specific scaling preferences as explored in Section 3.2. Additionally, we introduce a hybrid approach at Level 0, which selects the best-performing γ for each dataset. At Level 1, ZeroTuning uses uniform scaling across all heads with an optimized γ . At Level 2, it classifies attention heads, scales only the over-mixing or under-mixing heads, and searches for the optimal γ .

Table 5: Performance of ZeroTuning Under Different Resource Constraints.

| Method | Classification | | | | | | | Avg. Class. | Multiple Choice | | | | | | Avg. MC | |
|----------------------------|----------------|-------|-------|-------|-------|-------|-------|-------------|-----------------|-------|--------|--------|-------|-------|---------|-------|
| | SST-2 | SST-5 | MR | BoolQ | CB | TREC | SUBJ | | MMLU | AQUA | MathQA | LogiQA | CQA | PIQA | | |
| Vanilla | 73.20 | 45.40 | 89.20 | 69.60 | 82.14 | 14.00 | 44.60 | 59.73 | 67.40 | 25.69 | 33.60 | 39.40 | 77.60 | 83.60 | 84.62 | 58.84 |
| Level 0 ($\gamma = 2$) | 86.20 | 49.20 | 91.00 | 70.06 | 82.41 | 12.00 | 44.80 | 62.24 | 65.60 | 28.46 | 34.40 | 37.40 | 78.20 | 82.40 | 83.61 | 58.58 |
| Level 0 ($\gamma = 0.6$) | 53.80 | 43.40 | 82.40 | 72.00 | 83.93 | 17.20 | 44.60 | 56.76 | 67.00 | 22.53 | 32.60 | 40.20 | 77.60 | 82.60 | 83.61 | 58.02 |
| Level 0 (Hybrid) | 86.20 | 49.20 | 91.00 | 72.00 | 83.93 | 17.20 | 44.80 | 63.36 | 67.00 | 28.46 | 34.40 | 40.20 | 78.20 | 82.60 | 83.61 | 59.21 |
| Level 1 | 89.60 | 49.00 | 91.40 | 71.20 | 83.93 | 21.80 | 45.20 | 64.59 | 68.00 | 30.04 | 35.00 | 42.80 | 79.20 | 83.80 | 84.62 | 60.49 |
| Level 2 | 91.60 | 52.00 | 92.00 | 82.40 | 89.29 | 26.20 | 66.60 | 71.44 | 68.80 | 30.43 | 36.60 | 42.80 | 80.40 | 85.40 | 85.95 | 61.48 |

As shown in Table 5, ZeroTuning consistently improves performance across all resource levels. Even at Level 0, where resources are tightly constrained, the hybrid approach delivers steady gains over vanilla inference. These improvements become more substantial at Levels 1 and 2, where additional resources enable parameter optimization and head classification. Specifically, compared to the vanilla baseline, ZeroTuning increases average accuracy on text classification tasks by 3.63 percentage points at Level 0 (Hybrid), 4.86 percentage points at Level 1, and 11.71 percentage points at Level 2. For multiple-choice tasks, the corresponding gains are 0.37, 1.65, and 2.64 percentage points, respectively.

I SENSITIVITY TO DIFFERENT CONTEXT LENGTHS

To investigate how the distance between the initial token and task-relevant tokens affects model behavior, we evaluate the sensitivity of ZeroTuning under varying context lengths. Specifically, we insert task-irrelevant tokens between the initial token and the original input to artificially extend the context. This allows us to isolate the impact of increased token distance on attention and performance.

We conduct experiments using Llama-3.1-8B-Instruct and apply ZeroTuning with the same set of heads and scaling factors used in the previous base (non-extended) context setting. This ensures that any performance change is due solely to increased context length rather than re-optimized tuning parameters.

As shown in Table 6, the performance of vanilla LLMs consistently degrades as context length increases, likely due to disrupted information mixing caused by the inserted tokens. In contrast, ZeroTuning remains robust across all tested context lengths, yielding consistent and often significant improvements even under extreme cases of context extension. These results suggest that tuning the initial token’s attention can effectively stabilize information flow, even when relevant content is pushed further away in the input sequence.

J ROBUSTNESS ACROSS FEW-SHOT SCENARIOS

Few-shot learning has become a widely adopted approach to improve the performance of LLMs by providing a small number of in-context examples, enabling adaptation to specific tasks with minimal data (Brown et al., 2020). Building on previous zero-shot evaluations, we now evaluate the robustness of ZeroTuning in 1-shot and 2-shot scenarios across four datasets: SST-5, BoolQ, MMLU, and AQUA. To ensure consistency, we fix the randomly selected examples, maintain the selected head and scaling factor throughout the experiments.

The results in Table 7 show that ZeroTuning consistently outperforms the vanilla baseline across both 1-shot and 2-shot settings. In the 1-shot scenario, ZeroTuning achieves an average accuracy improvement of 1.85% over the vanilla model, with notable gains of 2.0% on BoolQ (82.40% vs. 80.40%) and 1.8% on SST-5 (49.40% vs. 47.60%). In the 2-shot scenario, the average improvement increases to 3.08%, with a significant 7.12% increase on AQUA (32.81% vs. 25.69%) and 2.0% on SST-5 (52.40% vs. 50.40%). Notably, ZeroTuning in the zero-shot setting outperforms vanilla few-

1512 Table 6: Impact of Context Length on ZeroTuning Performance.
1513

| 1514 Dataset | 1515 Method | 1516 Extra Context Length | | | 1517 Average | |
|--------------|-------------|---------------------------|--------------|--------------|--------------|--------------|
| | | 1518 0 | 1519 100 | 1520 200 | | |
| 1517 SST-2 | Vanilla | 73.20 | 68.40 | 59.20 | 32.00 | 58.20 |
| | ZeroTuning | 91.60 | 89.20 | 87.40 | 85.40 | 88.40 |
| | Diff | 18.40 | 20.80 | 28.20 | 53.40 | 30.20 |
| 1520 BoolQ | Vanilla | 69.60 | 68.60 | 67.60 | 68.60 | 68.60 |
| | ZeroTuning | 82.40 | 81.80 | 81.40 | 81.20 | 81.70 |
| | Diff | 12.80 | 13.20 | 13.80 | 12.60 | 13.10 |
| 1523 LogiQA | Vanilla | 39.40 | 36.60 | 36.20 | 35.80 | 37.00 |
| | ZeroTuning | 42.40 | 43.00 | 41.00 | 41.00 | 41.85 |
| | Diff | 3.00 | 6.40 | 4.80 | 5.20 | 4.85 |
| 1526 PIQA | Vanilla | 83.60 | 82.20 | 81.20 | 80.60 | 81.90 |
| | ZeroTuning | 85.40 | 83.80 | 83.20 | 82.80 | 83.80 |
| | Diff | 1.80 | 1.60 | 2.00 | 2.20 | 1.90 |

1528
1529 shot baselines, achieving higher accuracy without the additional context overhead and contextual
1530 biases introduced by in-context examples.

1532 Our results also highlight the following key findings:

1534 1. ZeroTuning improves LLM performance, even when few-shot learning does not benefit the
1535 base model. Most datasets show improvements with few-shot learning, likely due to clearer
1536 patterns and better output formatting. However, some datasets, like MMLU, experience
1537 performance drops, possibly due to increased confusion from the examples. Despite this,
1538 ZeroTuning still leads to consistent performance gains.

1539 2. Similar to Few-Shot Learning, ZeroTuning reduces invalid responses from LLMs, indicating
1540 improved instruction following. For instance, in the SST-2 dataset, LLMs sometimes
1541 output incorrect responses like “neutral” in zero-shot settings when they should respond
1542 with “positive” or “negative”. Few-shot learning helps the model understand the expected
1543 format, improving accuracy. Interestingly, ZeroTuning also reduces these errors, suggesting
1544 that it helps the model better understand task-relevant information.

1546 Table 7: Comparison of Vanilla and ZeroTuning Performance Across Few-Shot Learning Scenarios.
1547

| 1548 Shot | 1549 Method | 1550 SST-5 | 1551 BoolQ | 1552 MMLU | 1553 AQUA | 1554 Average |
|-------------|-------------|-------------|-------------|--------------|-------------|--------------|
| 1550 0-Shot | Vanilla | 45.4 | 69.6 | 67.4 | 25.7 | 52.0 |
| | ZeroTuning | 52.0 | 82.4 | 68.80 | 30.4 | 58.40 |
| | Diff | 6.6 | 12.8 | 1.4 | 4.7 | 6.4 |
| 1553 1-Shot | Vanilla | 47.6 | 80.4 | 61.8 | 28.1 | 54.5 |
| | ZeroTuning | 49.4 | 82.4 | 63.4 | 30.0 | 56.3 |
| | Diff | 1.8 | 2.0 | 1.6 | 1.9 | 1.8 |
| 1556 2-Shot | Vanilla | 50.4 | 83.4 | 64.4 | 25.7 | 56.0 |
| | ZeroTuning | 52.4 | 85.0 | 66.0 | 32.8 | 59.1 |
| | Diff | 2.0 | 1.6 | 1.6 | 7.1 | 3.1 |

1560 K IMPACT OF DECODING STRATEGIES

1562 Decoding strategies play a crucial role in shaping the output behavior of LLMs, and can influence
1563 performance across tasks. We evaluate the robustness of ZeroTuning over three strategies: Top-
1564 k Sampling, Top-p Sampling, and Beam Search, using Llama-3.1-8B on MMLU and SST-2, with
1565 results in Table 8.

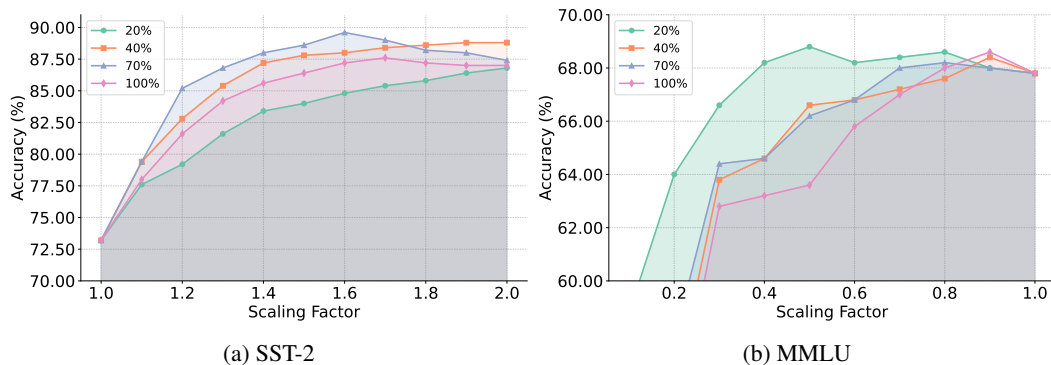
1566 Table 8: Performance Comparison Across Decoding Strategies with and without ZeroTuning on
 1567 MMLU and SST-2.

| Dataset | Method | Top- k Sampling | Top- p Sampling | Beam Search | Average |
|---------|------------|-------------------|-------------------|--------------|--------------|
| MMLU | Vanilla | 63.80 | 63.80 | 63.00 | 63.53 |
| | ZeroTuning | 65.80 | 66.00 | 65.20 | 65.67 |
| | Diff | 2.00 | 2.20 | 2.20 | 2.13 |
| SST-2 | Vanilla | 64.40 | 66.60 | 66.60 | 65.87 |
| | ZeroTuning | 89.20 | 89.60 | 89.20 | 89.33 |
| | Diff | 24.80 | 23.00 | 22.60 | 23.47 |

1576
 1577 Across all decoding strategies, ZeroTuning consistently improves over the vanilla baseline. On
 1579 MMLU, it yields performance gains of 2.0% with Top- k , 2.2% with Top- p , and 2.2% with Beam
 1580 Search, resulting in an average improvement of 2.1%. On SST-2, the improvements are even more
 1581 substantial: 24.8% with Top- k , 23.0% with Top- p , and 22.6% with Beam Search, with an average
 1582 gain of 23.5%.

L THE EFFECT OF DIFFERENT NUMBERS OF HEADS

1586 As shown in Figure 19, we observe that tuning an appropriate proportion of attention heads leads
 1587 to the best performance. Specifically, Figure 19a presents results on the SST-2 dataset, where we
 1588 tune the up-effective heads, while Figure 19b reports performance on the MMLU dataset with the
 1589 down-effective heads. Across both datasets, we find that tuning a moderate proportion of heads
 1590 (typically between 40% and 70%) achieves the highest accuracy. In contrast, tuning too few or too
 1591 many heads tends to degrade performance, suggesting that selective head tuning is key to effective
 1592 inference-time adaptation.



1605 Figure 18: Accuracy of tuning different proportions of heads. (a) SST-2: tuning up-effective heads;
 1606 (b) MMLU: tuning down-effective heads.

1620 M SENSITIVITY TO PROMPT VARIATIONS

1622 Prompts play a crucial role in guiding LLM behavior and typically consist of three components:
 1623 **Instruction1** (task guidance), **Question** (the actual query), and **Instruction2** (output format spec-
 1624 ification). To evaluate the robustness of ZeroTuning under prompt perturbations, we perform ex-
 1625 periments on the LLaMA-3.1-8B model using MMLU and SST-2 under three prompt formats: Full
 1626 Prompt (Instruction1 + Question + Choices + Instruction2), Drop Instruction1, and Modify Instruc-
 1627 tion2. Detailed prompt examples are provided in Appendix O.

1628 As shown in Table 9, ZeroTuning consistently improves performance across all prompt configu-
 1629 rations, and maintains strong performance even when key instructions are modified or omitted,
 1630 demonstrating its distinctive ability to regulate and adapt to prompt variations. On MMLU, the
 1631 performance gains range from 1.2% to 2.4%, with an average improvement of 1.7%. On SST-2, the
 1632 gains are more substantial, ranging from 24.8% to 26.2%, with an average improvement of 25.3%.

1633 Table 9: Effect of Prompt Variations on Performance with and without ZEROTUNING.

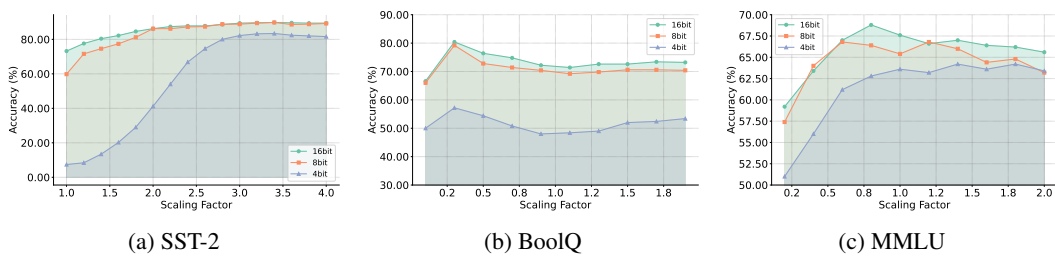
| Prompt Format | Method | MMLU | SST-2 | Average |
|---------------------|------------|--------------|--------------|--------------|
| Full Prompt | Vanilla | 67.40 | 64.40 | 65.90 |
| | ZeroTuning | 68.80 | 89.20 | 79.00 |
| | Diff | 1.4 | 24.8 | 13.1 |
| Drop Instruction1 | Vanilla | 66.80 | 64.40 | 65.60 |
| | ZeroTuning | 68.00 | 89.20 | 78.60 |
| | Diff | 1.2 | 24.8 | 13.0 |
| Modify Instruction2 | Vanilla | 61.80 | 61.80 | 61.80 |
| | ZeroTuning | 64.20 | 88.00 | 76.10 |
| | Diff | 2.4 | 26.2 | 14.3 |

1647 N THE EFFECT OF DIFFERENT QUANTIZATION CONFIGURATIONS

1649 As shown in Figure 19, we observe:

1651 (a) Quantizing to 8-bit results in only a slight accuracy decrease compared to 16-bit, while 4-bit
 1652 quantization leads to a significant accuracy decrease. However, by appropriately tuning attention to
 1653 the initial token, we find that the best accuracy with 8-bit quantization becomes comparable to that
 1654 of the 16-bit model on the SST-2 and BoolQ datasets. This suggests that our method can partially
 1655 compensate for the performance loss caused by quantization.

1656 (c) The accuracy trends across different quantization levels are largely similar. This consistency
 1657 may offer useful insights for future work, for instance, searching for optimal parameters using low-
 1658 precision models and transferring them to higher-precision models.



1668 Figure 19: Accuracy when tuning under different quantization configurations.

1674 **O PROMPTS USED FOR EACH DATASET**
16751676 Here, we list all the prompts we used in this paper on different datasets:
16771678 For multiple-choice task, we use the following prompt:
16791680 **Prompt for Multiple-Choice Tasks**1681 Generate the correct answer to the following question.
1682 <Question>
1683 <choice 1>
1684 <choice 2>
1685 <choice 3>
1686 ...
1687 Answer:"1688 For text classification, we use different prompts for different datasets.
16891690 **Prompt for SST-2**1691 "Classify the sentiment of the user's message into one of the following categories: 'positive'
1692 or 'negative'.
1693 Sentence: <sentence>
1694 Sentiment: "1695 **Prompt for SST-5**1696 "Classify the sentiment of the user's message into one of the following categories: 'terrible',
1697 'negative', 'neutral', 'positive', or 'great'.
1698 Sentence: <sentence>
1699 Sentiment: "1700 **Prompt for MR**1701 "Classify the sentiment of the movie's review into one of the following categories: 'positive'
1702 or 'negative'.
1703 Review: <sentence>
1704 Sentiment: "1705 **Prompt for TREC**1706 "Classify the given questions into the following categories: 'Description', 'Entity', 'Expres-
1707 sion', 'Person', 'Number', or 'Location'.
1708 Question: <sentence>
1709 Type: "1710 **Prompt for CB**1711 "Read the following paragraph and determine if the hypothesis is true.
1712 Premise: <premise> Hypothesis: <hypothesis>.
1713 Answer: "1714 **Prompt for BoolQ**1715 "Read the text and answer the question by True or False.
1716 Text: <passage> Question: <question>?
1717 Answer: "

1728

1729

1730

Prompt for SUBJ

”Classify the input into one of the following categories: subjective or objective.

Input: <text>

Category: ”

1733

1734

P PROMPT FOR KEY TOKENS IDENTIFICATION

1735

1736

1737

Prompt for key tokens identification

1738

Below is a question. Please extract the key content words or phrases from the question that are crucial for understanding and answering it correctly. These are typically the nouns, verbs, adjectives, or multi-word expressions that define the subject, action, or relation in the question. Output your selection as a Python list, where each element is a word or a phrase enclosed in quotes.

For example, for the question 'What is the boiling point of water?', the key words might be ['boiling point', 'water'].

Question: {question}

Key Words:

1747

1748

STATEMENT ON LARGE LANGUAGE MODEL USAGE

1749

1750

1751

In adherence to the ICLR 2026 policy, we report the use of Large Language Models (LLMs) during the preparation of this paper. The primary applications were to aid and polish the writing. Specifically, an LLM was utilized to improve sentence structure, enhance clarity, ensure grammatical accuracy, and rephrase text for conciseness and impact. Additionally, the LLM assisted in research discovery by summarizing provided academic papers and helping to structure the literature survey.

1756

1757

1758

1759

All core scientific contributions—including the formulation of the central hypothesis, the design and execution of experiments, the analysis of data, and the final conclusions—are the original work of the human authors. The LLM’s role was strictly that of a sophisticated writing and research assistant.

1760

1761

1762

1763

1764

1765

1766

1767

1768

1769

1770

1771

1772

1773

1774

1775

1776

1777

1778

1779

1780

1781